AD-A193 576 EPIC-2 PREDICTED SHOCK ENVIRONMENTS IN ROLLED HOMOGENEOUS ARMOR FOR NONPE..(U) ARMY BALLISTIC RESEARCH LAB ABERDEEN PROVING GROUND MD E F QUIGLEY 1/1

UNCLASSIFIED JAN 88 BRL-TR-2886 F/G 19/4 NL

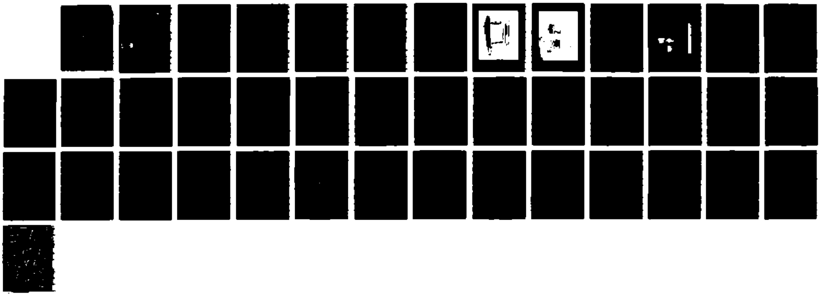

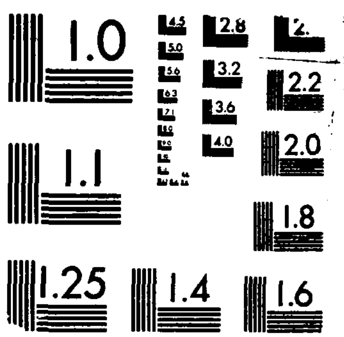

MICROCOPY RESOLUTION TEST CHART
UREAU [illegible] STANDARDS-1963-A

(4)

AD

TECHNICAL REPORT BRL-TR-2886

EPIC-2 PREDICTED SHOCK ENVIRONMENTS IN ROLLED HOMOGENEOUS ARMOR FOR NONPERFORATING BALLISTIC IMPACT

ENNIS F. QUIGLEY

JANUARY 1988

US ARMY BALLISTIC RESEARCH LABORATORY
ABERDEEN PROVING GROUND, MARYLAND

DESTRUCTION NOTICE

Destroy this report when it is no longer needed. DO NOT return it to the originator.

Additional copies of this report may be obtained from the National Technical Information Service, U.S. Department of Commerce, Springfield, VA 22161.

The findings of this report are not to be construed as an official Department of the Army position, unless so designated by other authorized documents.

The use of trade names or manufacturers' names in this report does not constitute indorsement of any commercial product.

SECURITY CLASSIFICATION OF THIS PAGE

ADA193576

REPORT DOCUMENTATION PAGE

Form Approved OMB No 0704-0188 Exp. Date Jun 30, 1986

1a. REPORT SECURITY CLASSIFICATION: Unclassified	1b. RESTRICTIVE MARKINGS
2a. SECURITY CLASSIFICATION AUTHORITY	3. DISTRIBUTION/AVAILABILITY OF REPORT: Approved for public release; distribution unlimited
2b. DECLASSIFICATION/DOWNGRADING SCHEDULE	
4. PERFORMING ORGANIZATION REPORT NUMBER(S): BRL-TR-2886	5. MONITORING ORGANIZATION REPORT NUMBER(S)
6a. NAME OF PERFORMING ORGANIZATION: US Army Ballistic Research Laboratoty; 6b. OFFICE SYMBOL (If applicable): SLCBR-VL-V	7a. NAME OF MONITORING ORGANIZATION
6c. ADDRESS (City, State, and ZIP Code): Aberdeen Proving Ground, MD 21005-5066	7b. ADDRESS (City, State, and ZIP Code)
8a. NAME OF FUNDING/SPONSORING ORGANIZATION; 8b. OFFICE SYMBOL (If applicable)	9. PROCUREMENT INSTRUMENT IDENTIFICATION NUMBER
8c. ADDRESS (City, State, and ZIP Code)	10. SOURCE OF FUNDING NUMBERS: PROGRAM ELEMENT NO. / PROJECT NO. / TASK NO. / WORK UNIT ACCESSION NO

11. TITLE (Include Security Classification)
EPIC-2 PREDICTED SHOCK ENVIRONMENTS IN ROLLED HOMOGENEOUS ARMOR FOR NONPERFORATING BALLISTIC IMPACT

12. PERSONAL AUTHOR(S)
Quigley, Ennis F.

13a. TYPE OF REPORT	13b. TIME COVERED FROM ____ TO ____	14. DATE OF REPORT (Year, Month, Day)	15. PAGE COUNT

16. SUPPLEMENTARY NOTATION

17. COSATI CODES		
FIELD	GROUP	SUB-GROUP

18. SUBJECT TERMS (Continue on reverse if necessary and identify by block number)
EPIC-2, Rolled homogeneous armor, Nonperforation, Ballistic impact, Penetration mechanics, Computer simulation, Shock

19. ABSTRACT (Continue on reverse if necessary and identify by block number)

A series of controlled experiments were conducted to characterize the ballistic shock environment produced in rolled homogeneous armor by nonperforating ballistic impact. Displacements, velocities, accelerations and strains were measured at various locations on the back of 38 and 70 mm thick, 914 mm x 914 mm plates impacted by ball bearings and small caliber projectiles (30 caliber to 20 mm). Projectile impact velocities ranged from 335 m/s to 1508 m/s. Peak displacement measurements obtained for projectile impact agreed well with simple momentum predictions. However, velocity and acceleration measurements were inconsistent and a number of accelerometers were destroyed. Because of these measurement difficulties, the EPIC-2 hydro-code was used to calculate the plate velocity and acceleration distributions for the impact of the 20 mm projectile at impact velocities of 366, 1012 and 1508 m/s. Plate displacements, velocities, accelerations and strains were calculated for a 300 μs time period and comparison of measured and calculated displacements and strains for the three impact velocities showed good to excellent agreement. Maximum calculated accelerations below the impact point on the back surface of the plates ranged from 500,000 g's to 4,000,000 g's.

20. DISTRIBUTION/AVAILABILITY OF ABSTRACT: ☐ UNCLASSIFIED/UNLIMITED ☒ SAME AS RPT. ☐ DTIC USERS	21. ABSTRACT SECURITY CLASSIFICATION: Unclassified
22a. NAME OF RESPONSIBLE INDIVIDUAL: Ennis F. Quigley	22b. TELEPHONE (Include Area Code): (301) 278-6651; 22c. OFFICE SYMBOL: SLCBR-VL-V

DD FORM 1473, 84 MAR — 83 APR edition may be used until exhausted. All other editions are obsolete.

SECURITY CLASSIFICATION OF THIS PAGE

TABLE OF CONTENTS

LIST OF FIGURES

I. INTRODUCTION

A series of controlled experiments[1,2] were conducted by the US Army Combat Systems Test Activity, Aberdeen Proving Ground, MD to characterize the ballistic shock environment produced in rolled homogeneous armor (RHA) by nonperforating ballistic impact. Displacements, velocities, accelerations and strains were measured at various locations on the back of 914 mm x 914 mm x 38 mm and 914 mm x 914 mm x 70 mm RHA plates impacted by small caliber projectiles (30 caliber to 20 mm). Projectile impact velocities ranged from 335 m/s to 1508 m/s. Although peak displacement measurements obtained agreed well with simple momentum predictions, velocity and acceleration measurements were inconsistent and a number of accelerometers were destroyed. Because of these measurement difficulties, the EPIC-2 hydrocode[3] was used to calculate the plate velocity and acceleration distributions for the impact of the 20 mm steel projectile at impact velocities of 366, 1012 and 1508 m/s. This report presents the results of the EPIC-2 calculations.

II. BALLISTIC IMPACT EXPERIMENT

Figure 1 is a photograph of one of the test plates bolted to the support structure. Eighteen bolts were used to attach the plate to the structure. The plate was mechanically and electrically isolated from the structure by two dissimilar materials (aluminum and fiber glass) placed between the plate and the bolting bars. The ball-peen and sledge hammers in the photograph were used to check out the instrumentation. Also seen in the photograph is a 50 mm diameter ball bearing used in one of the experiments.

Displacements were measured using commercial, non-contacting eddy-current probes and a locally fabricated, capacitive displacement transducer. Velocity transducers supplied by the Naval Ship Research and Development Center were used to measure the plate velocities. Three different models of piezoresistive accelerometers were used to measure accelerations. Conventional foil-type and semi-conductor type strain gages were used to measure strain. The acceleration, velocity and strain transducers were attached to the plate while the displacement transducers were mounted on a transducer support frame directly behind the plate. Figure 2 is a photograph showing the transducers on the back of the plate and Figure 3 is a diagram of the locations of those transducers to the left of the impact point as seen from the back of the plate.

Figure 4 shows the 20 mm projectile before and after impact for the three impact velocities. The single projectile on the left is the "before". There was some plastic deformation but no material loss for the 366 m/s velocity. For the 1012 m/s velocity there was considerable plastic deformation and material loss. At 1508 m/s, the experimentalist could find nothing remaining of the projectile.

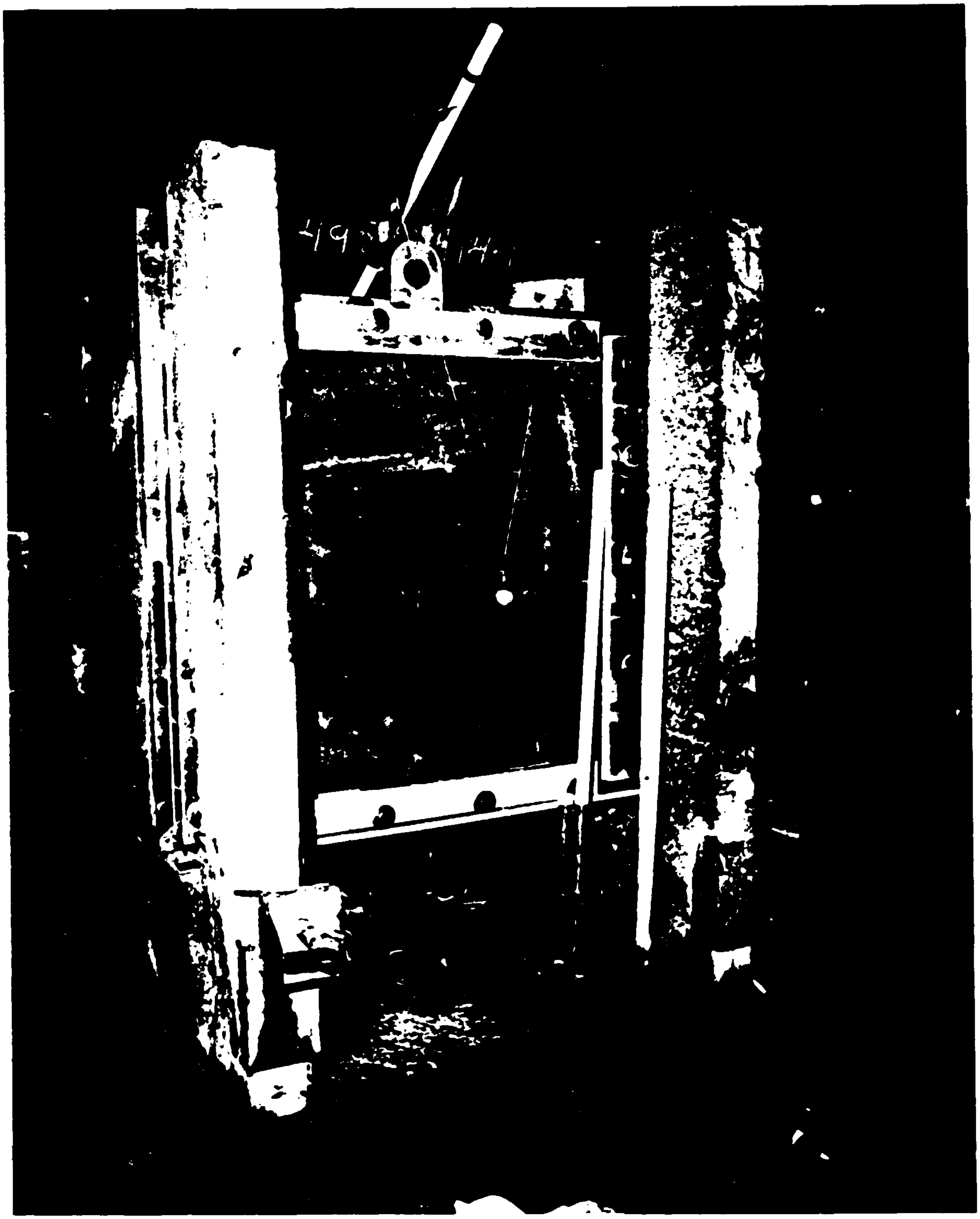

Figure 1. Photograph of RHA plate bolted to support structure.

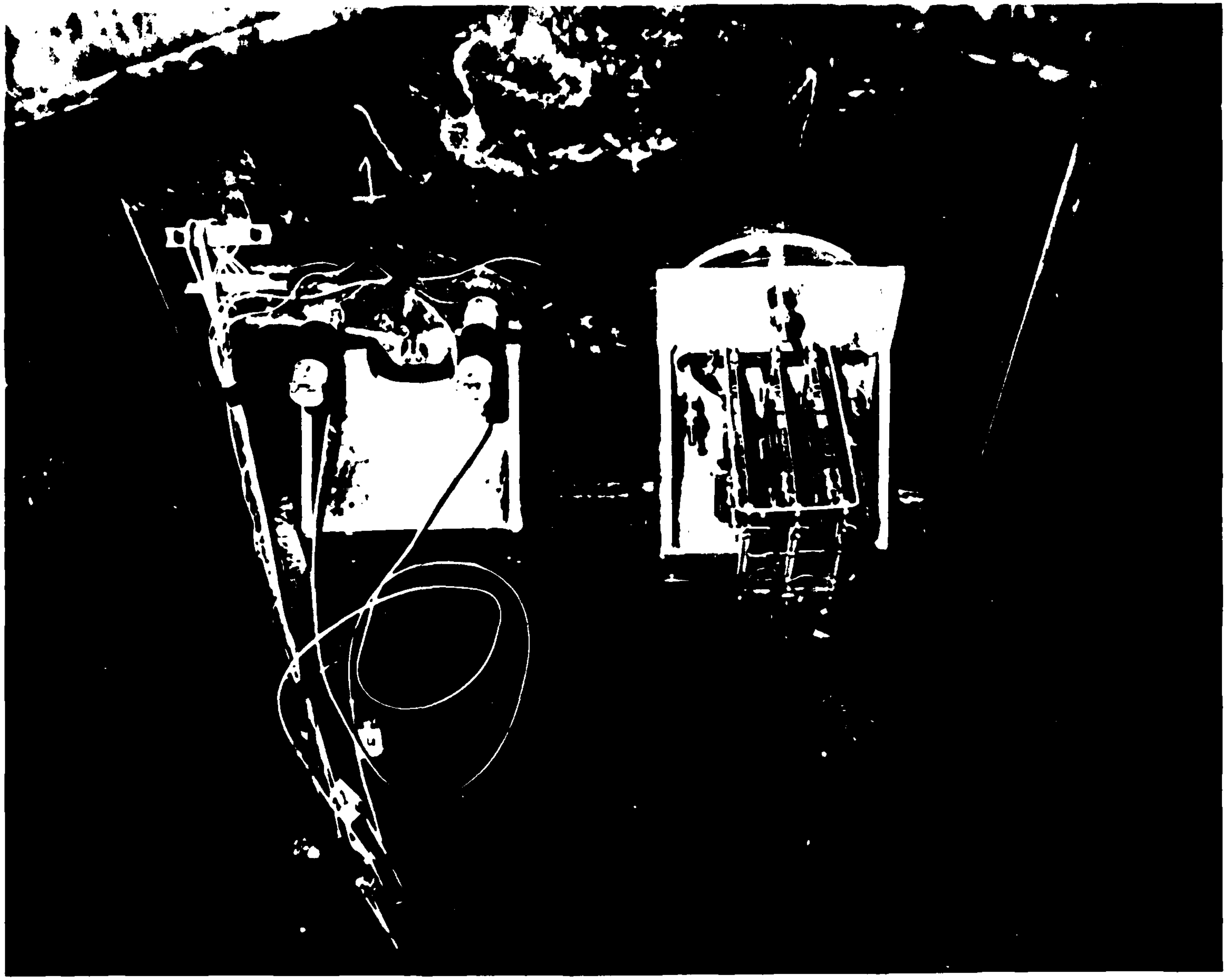

Figure 2. Photograph of transducers on back of plate.

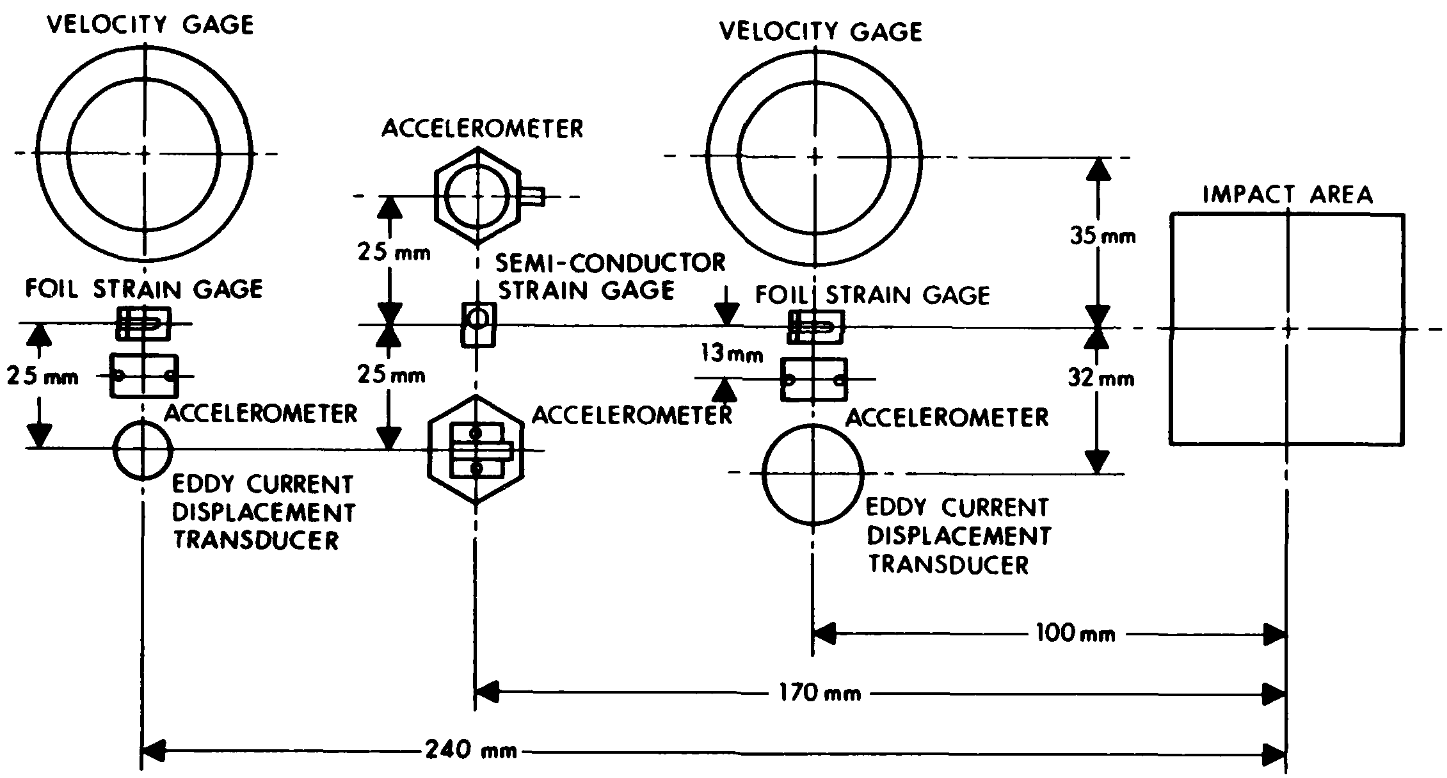

Figure 3. Location of transducers to the left of the impact area.

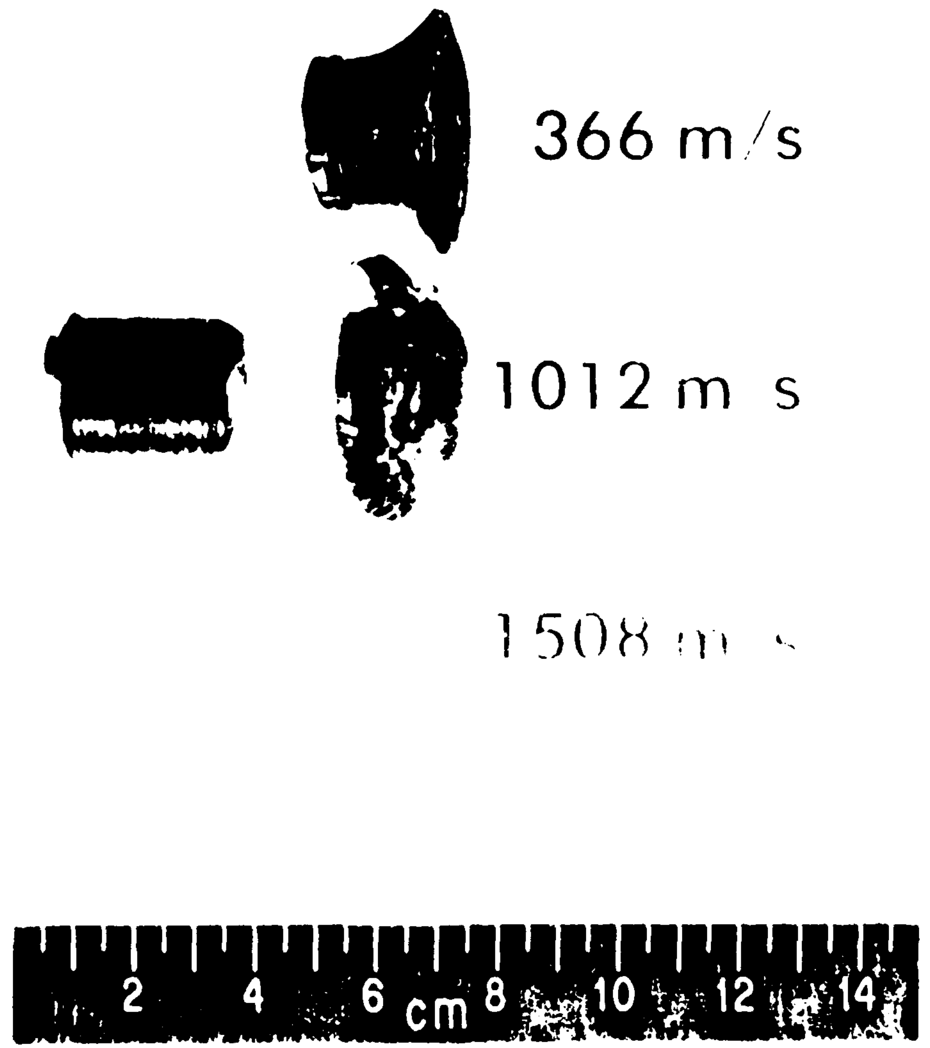

Figure 4. Photograph of projectile before and after impact.

III. THE EPIC-2 CODE CALCULATIONS

The major characteristics of the EPIC-2 code are listed in Table 1. The code performs elastic-plastic impact computations in two dimensions for axisymmetric and plane strain problems with either free or fixed boundaries. It is based on a Lagrangian finite element and lumped mass formulation in which the equations of motion are integrated directly. Nonlinear material strength and compressibility effects are included to account for elastic-plastic flow and wave propagation. The code has material descriptions for strain hardening, strain rate effects, thermal softening and failure. It uses a constant strain, triangular finite element which is well suited to represent the severe distortions occurring during high velocity impact.

The finite element models of the projectile and the 38 mm thick plate are shown in Figure 5. The projectile consisted of 84 elements and 57 nodes. The horizontal distance between the nodes was 2.54 mm and the vertical distance between the nodes ranged from 1.9 mm to 4.45 mm. The bolted, square plates were modeled as circular ones, 914 mm in diameter with free boundaries. Only the first 100 mm of the plate's 457 mm radius is shown. The 38 mm thick plate consisted of 671 nodes and 1200 elements and the 70 mm plate consisted of 1037 nodes and 1920 elements. Both the horizontal and vertical distances between the nodes were 7.62 mm. The material properties of the projectile and the plates used in the calculations are listed in Table 2.

The use of an axisymmetric code to model the experiments was justified since the impact point in the experiments was the center of a square plate. The plate's response for a brief period of time after impact would be axisymmetric and independent of the plate's geometry and edge boundary conditions. The times calculated for the dilatation and shear waves to travel the shortest round trip distance between the impact point and the plate's edges were 157 μs and 285 μs, respectively. Plate displacements, velocities, accelerations and strains were calculated for the first 300 μs after impact. Comparison of calculated axial displacements at a point 240 mm out from the impact point for free and fixed edges showed identical plate responses for times less than 215 μs. Comparison of calculated radial strains at the same location showed identical response for times less than 125 μs and minor differences in the response for times greater than 125 μs.

Because EPIC-2 calculates strain rates and not strains per se, the radial strains were calculated from the EPIC-2 calculated normal stresses using

$$\epsilon_{rr} = E^{-1}[\sigma_{rr}-\nu\{\sigma_{\theta\theta}+\sigma_{zz}\}]$$

where ϵ_{rr} is the radial strain, σ_{rr} is the radial stress, $\sigma_{\theta\theta}$ is the tangential stress and σ_{zz} is the axial stress. The values of Young's Modulus, E, and Poisson's ratio, ν, used in the calculations were $2.041\text{x}10^7$ Ncm^{-2} and 0.275, respectively.

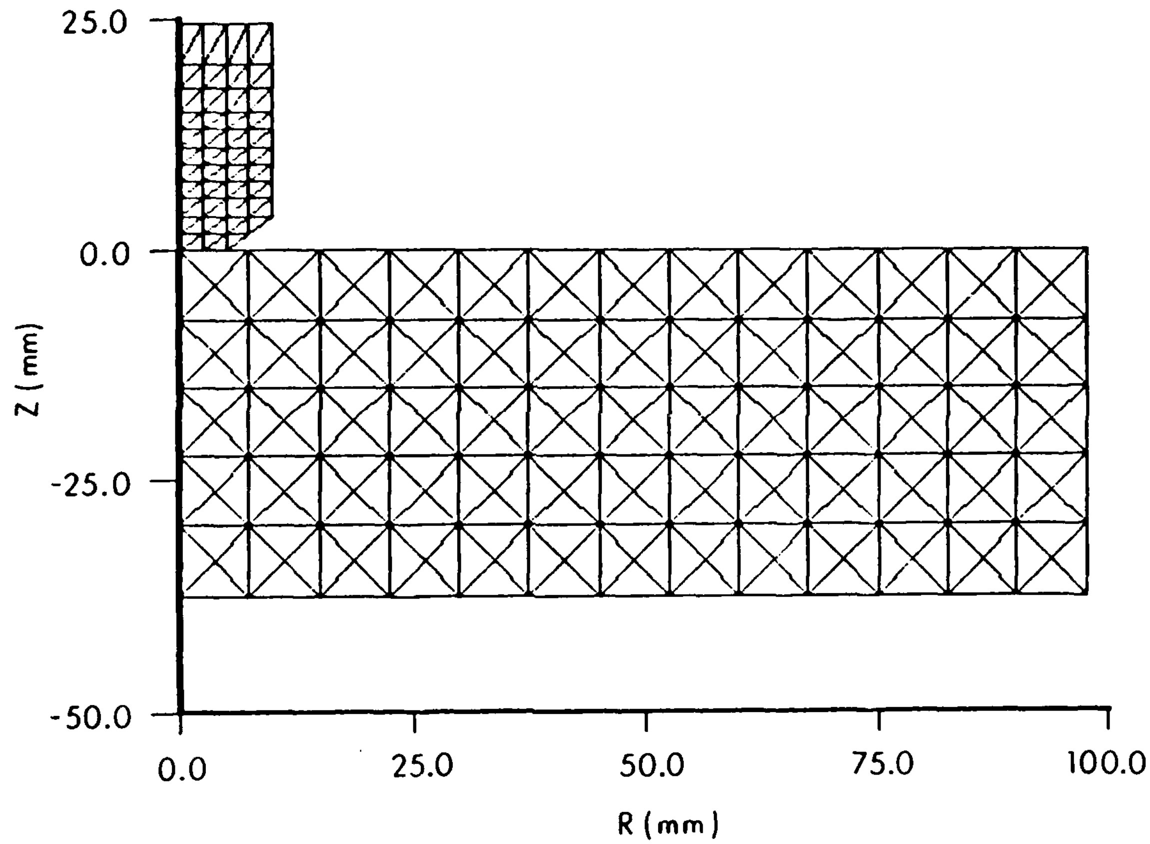

Figure 5. Finite element model of projectile and plate.

Table 1. EPIC-2 Code Characteristics	
DISCRETIZATION:	FINITE ELEMENT METHOD • 2D constant strain triangles • Lumped mass formulation
MESH DESCRIPTION:	LAGRANGIAN
MATERIAL MODEL:	CONSTITUTIVE MODEL • Incremental elastic-plastic • Von Mises yield criterion • Compressibility effects • Strain rate effects • Strain hardening • Thermal softening EQUATION OF STATE • Mie-Gruneisen • Ideal gas
FAILURE CRITERIA:	VOLUMETRIC STRAIN EFFECTIVE PLASTIC STRAIN
POST-FAILURE MODELS:	PRESSURE CUTOFF SHEAR AND TENSION FAILURE TOTAL FAILURE

IV. COMPARISON OF CALCULATED AND MEASURED RESPONSES

Figures 6 through 19 are plots of the calculated and measured plate response histories at the 100 mm, 170 mm and 240 mm transducer locations (see Figure 3) for the first 300 μs. Figures 6 through 10 are the responses for the 38 mm thick plate for the impact velocity of 366 m/s. Figures 11 through 15 are for the same plate thickness for the 1012 m/s impact velocity. Figures 16 through 19 are for the 70 mm thick plate for the impact velocity of 1508 m/s. Comparisons of the calculated and the measured plate's responses were made for the first 250 μs.

Table 2. Material Properties		
Property	**Projectile**	**Plate**
Density (Ns^2cm^{-2})	7.840×10^{-5}	7.904×10^{-5}
Specific heat ($cm^2s^{-2}K^{-1}$)	4.770×10^6	4.523×10^6
Shear modulus (Ncm^{-2})	7.752×10^6	8.019×10^6
Viscosity ($Nscm^{-2}$)	0.0	0.0
Yield stress (Ncm^{-2})	1.103×10^5	9.162×10^4
Ultimate stress (Ncm^{-2})	1.103×10^5	1.032×10^5
Ultimate strain	0.18	0.165
Maximum negative pressure (Ncm^{-2})	6.897×10^6	6.897×10^6
Strength equation		
Strain rate coefficient	0.0	0
1st pressure coefficient	0.0	0.0
2nd pressure coefficient	0.0	0.0
1st temperature coefficient	1.0	1.0
2nd temperature coefficient	0.0	0.0
Equation of state		
1st pressure coefficient (Ncm^{-2})	1.640×10^7	1.590×10^7
2nd pressure coefficient (Ncm^{-2})	2.944×10^7	5.170×10^7
3rd pressure coefficient (Ncm^{-2})	5.000×10^7	5.216×10^8
Gruneisen coefficient	1.16	1.69
Artificial viscosity equation		
Linear coefficient	0.2	0.2
Quadratic coefficient	4.0	4.0
Shear and tensile failure		
Equivalent strain	9.99×10^2	9.99×10^2
Volumetric strain	9.99×10^2	9.99×10^2
Total failure		
Equivalent strain	1.8	9.99×10^2
Initial temperature (K)	2.94×10^2	2.94×10^2

Zero times of the measured axial displacements were not at the time of impact and did not correspond to the zero time of the calculated displacements. In order to compare the data, zero time for the measured data was adjusted to give the best agreement with the calculated data. The agreement in Figure 6 is good whereas the agreement in Figures 7, 11, 12 and 16 is very good. The sign of the calculated displacements was inverted to agree with the positive displacement direction of the measured data.

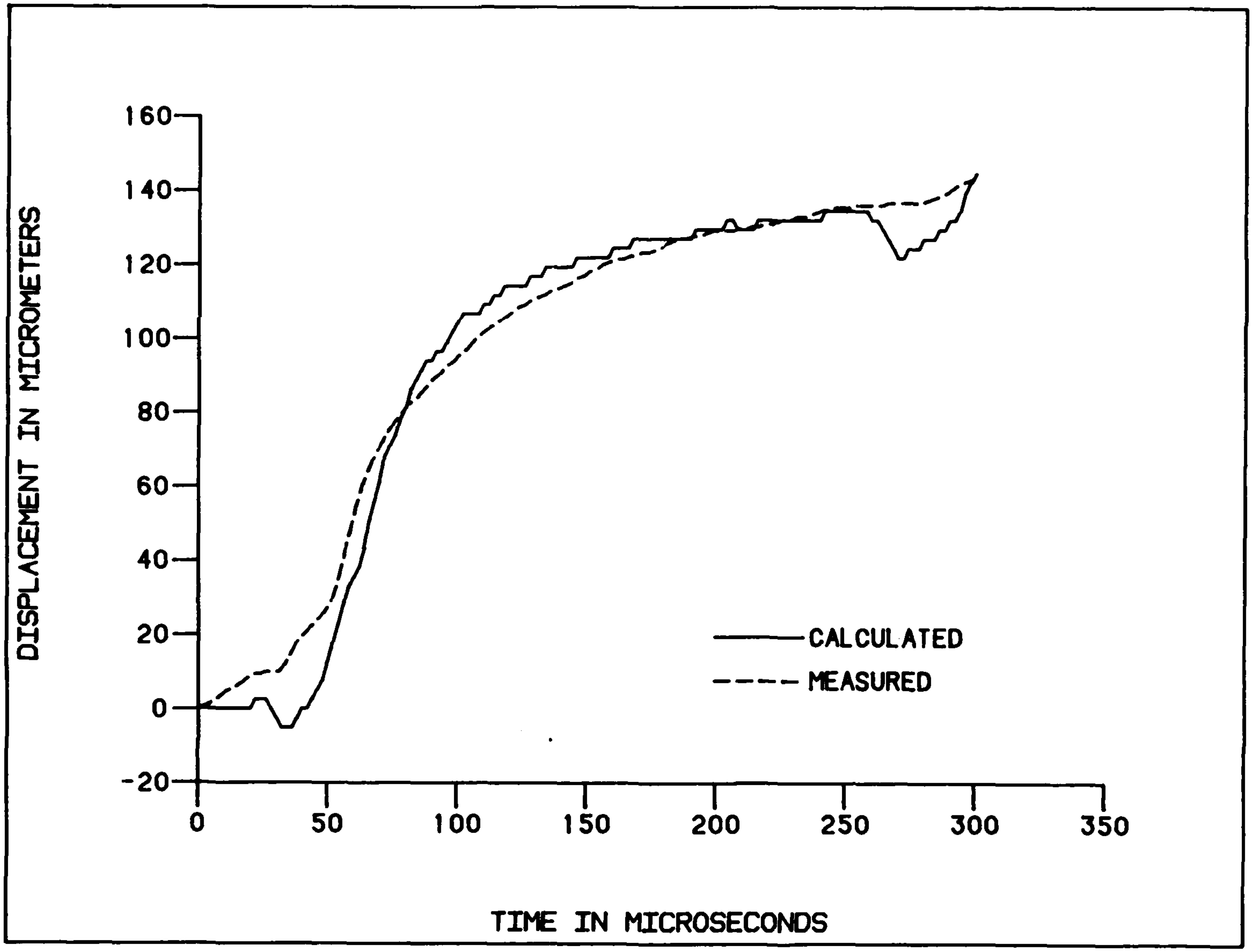

Figure 6. Axial displacement histories of 38 mm thick plate at 100 mm location for projectile impact velocity of 366 m/s.

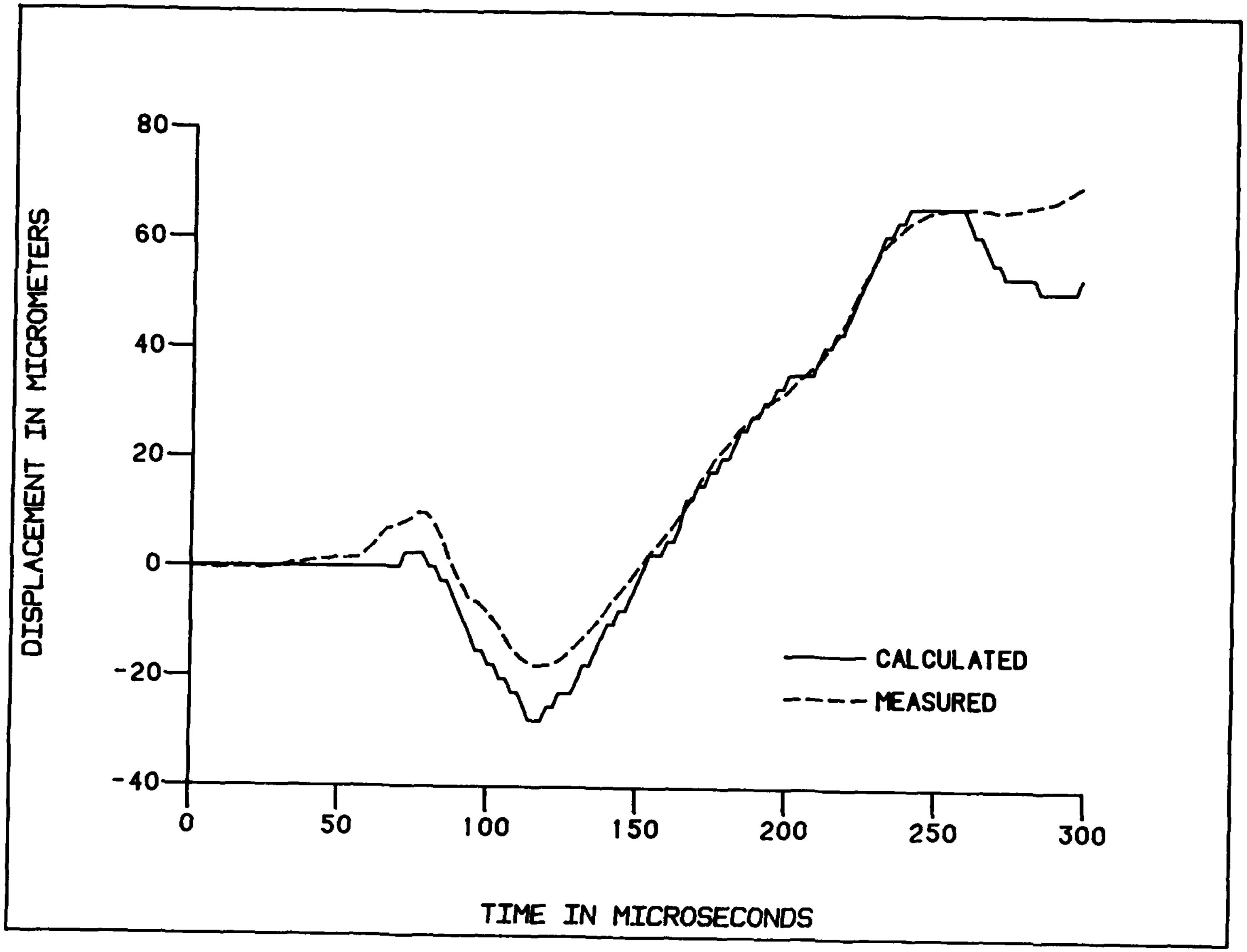

Figure 7. Axial displacement histories of 38 mm thick plate at 240 mm location for projectile impact velocity of 366 m/s.

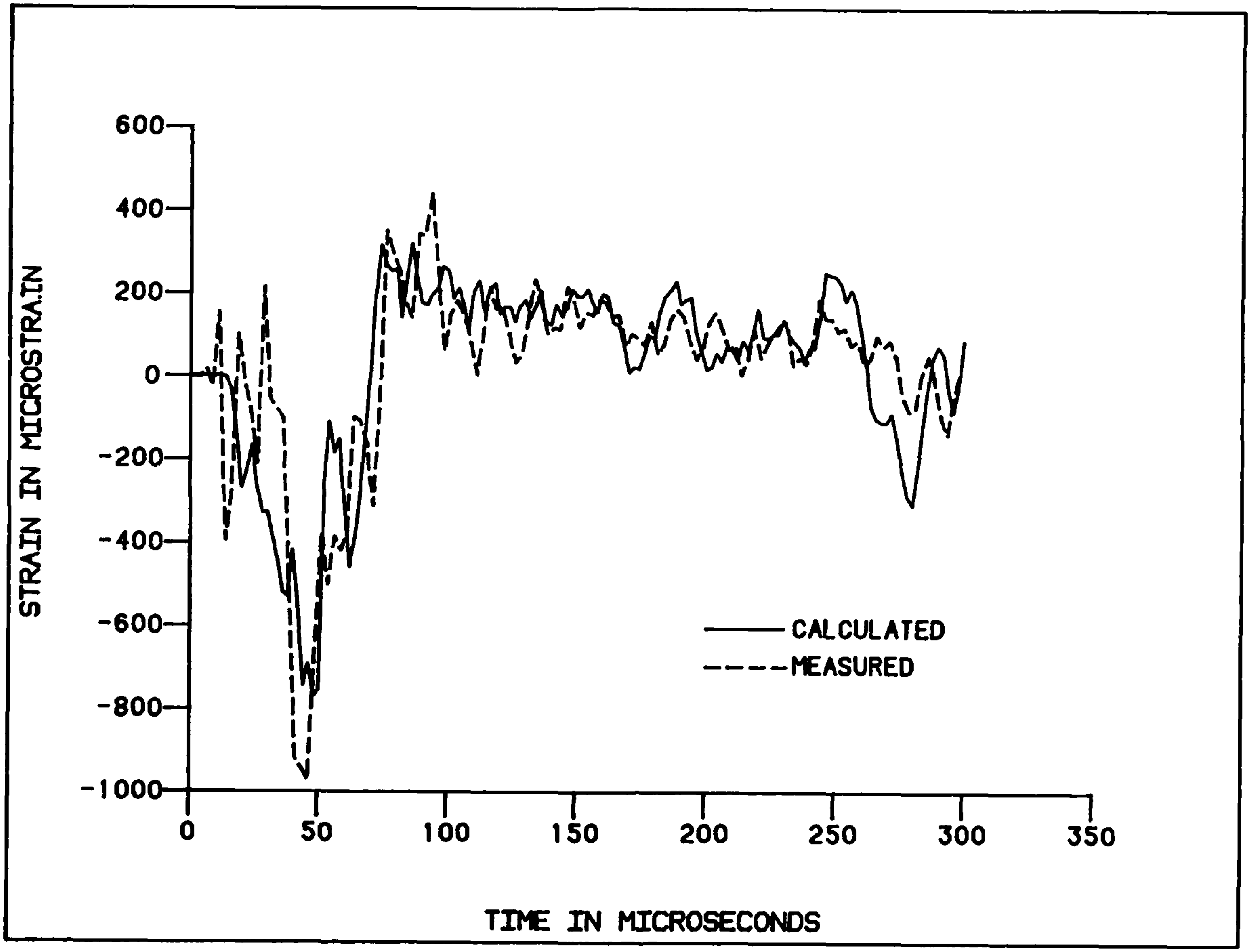

Figure 8. Radial strain histories of 38 mm thick plate at 100 mm location for projectile impact velocity of 366 m/s.

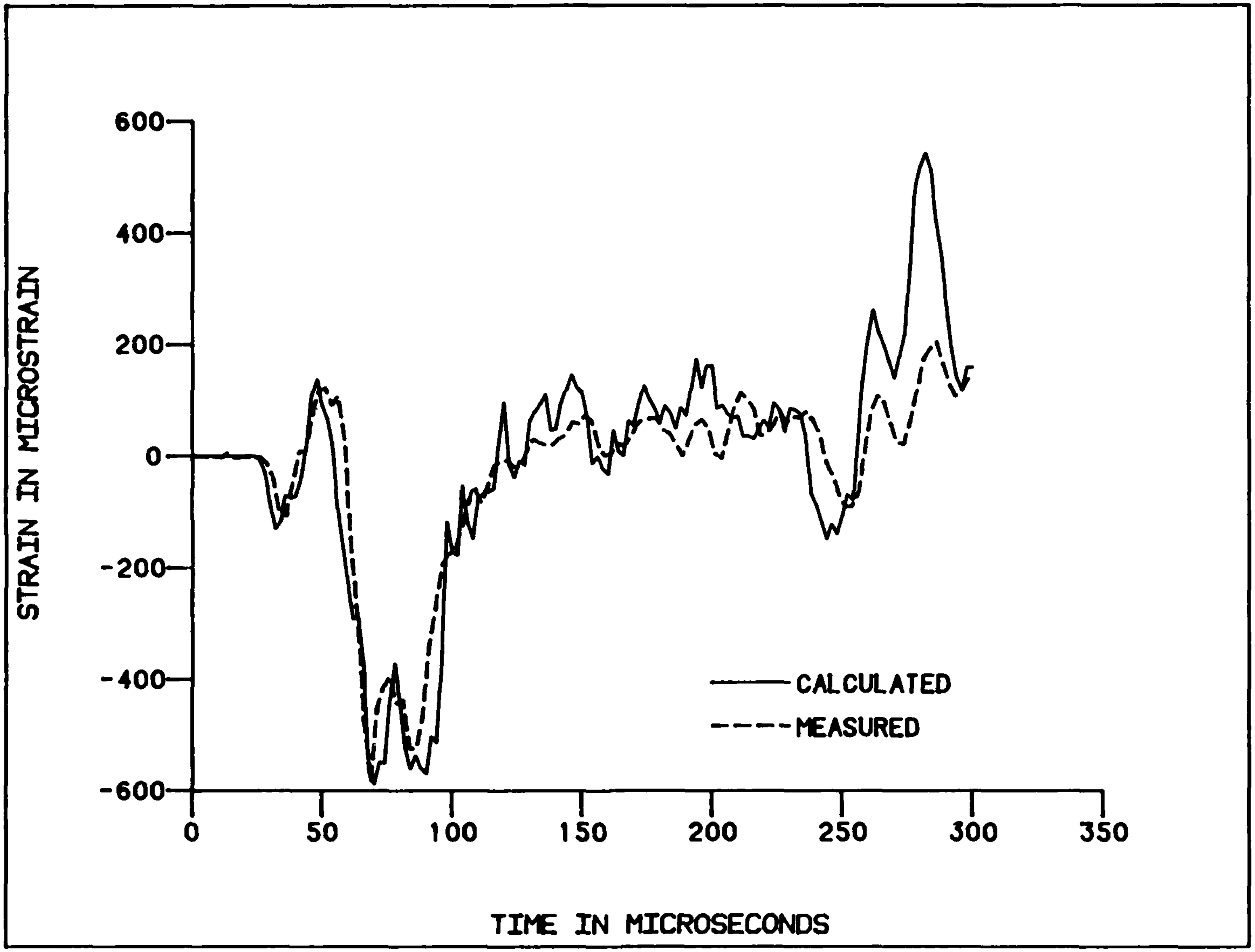

Figure 9. Radial strain histories of 38 mm thick plate at 170 mm location for projectile impact velocity of 366 m/s.

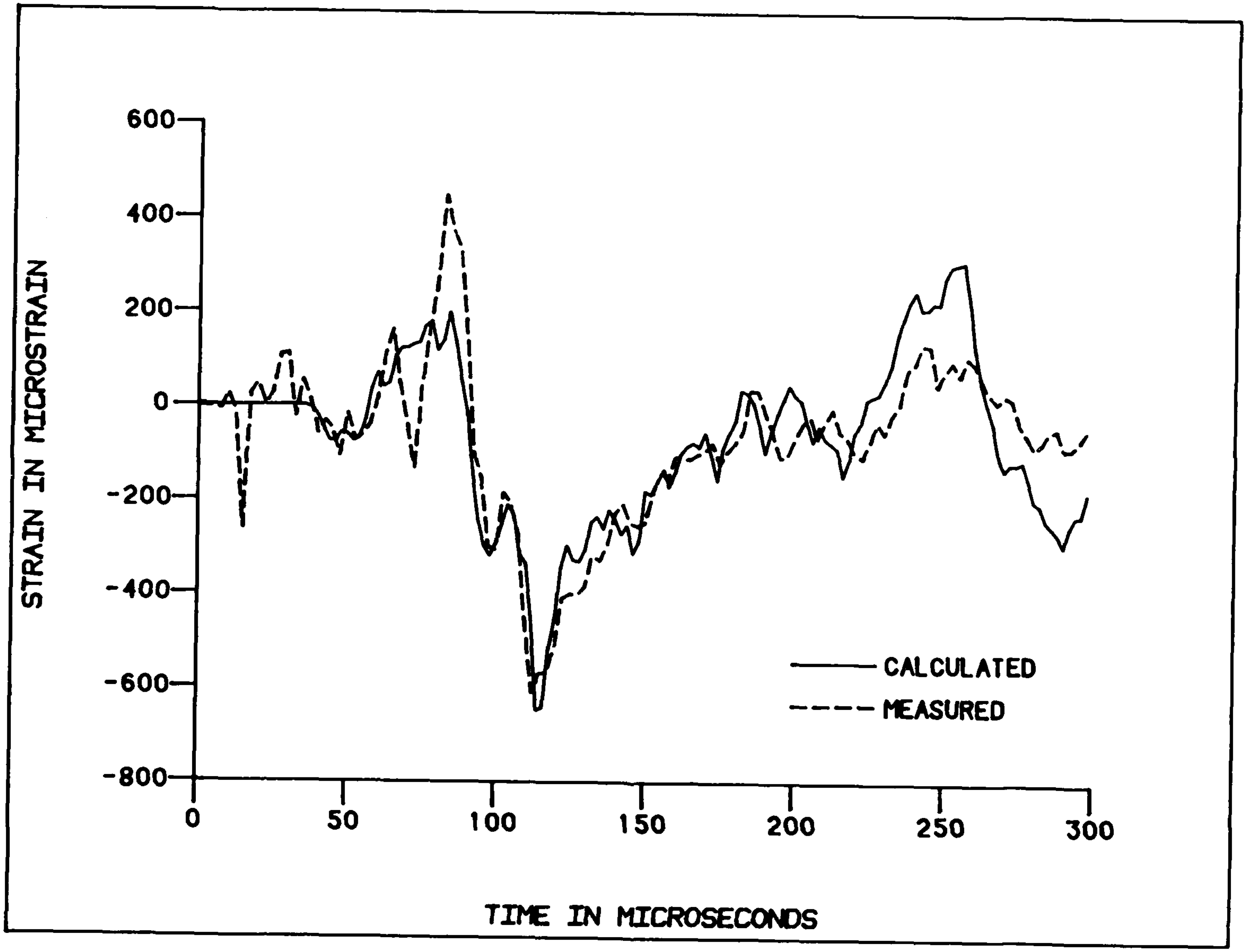

Figure 10. Radial strain histories of 38 mm thick plate at 240 mm location for projectile impact velocity of 366 m/s.

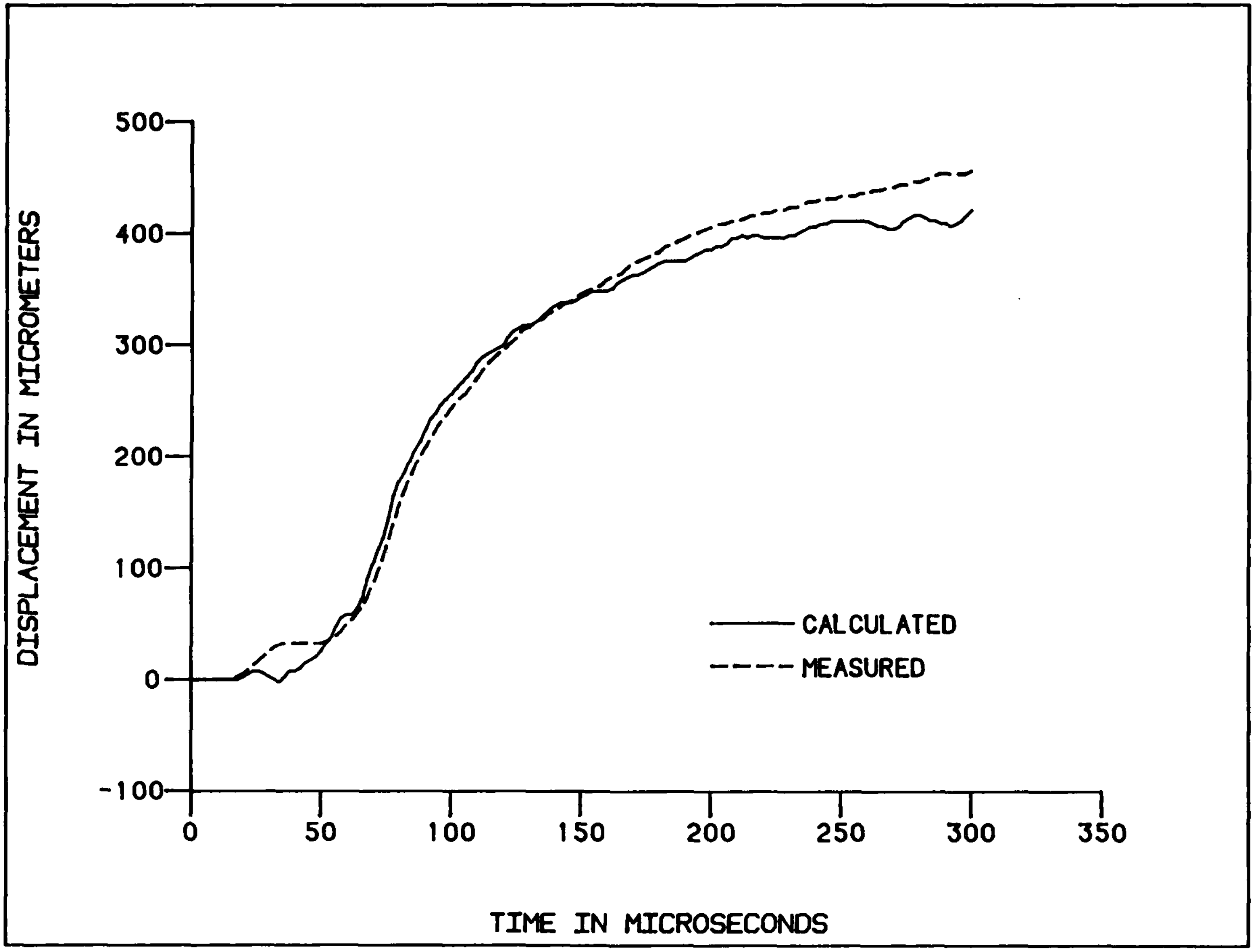

Figure 11. Axial displacement histories of 38 mm thick plate at 100 mm location for projectile impact velocity of 1012 m/s.

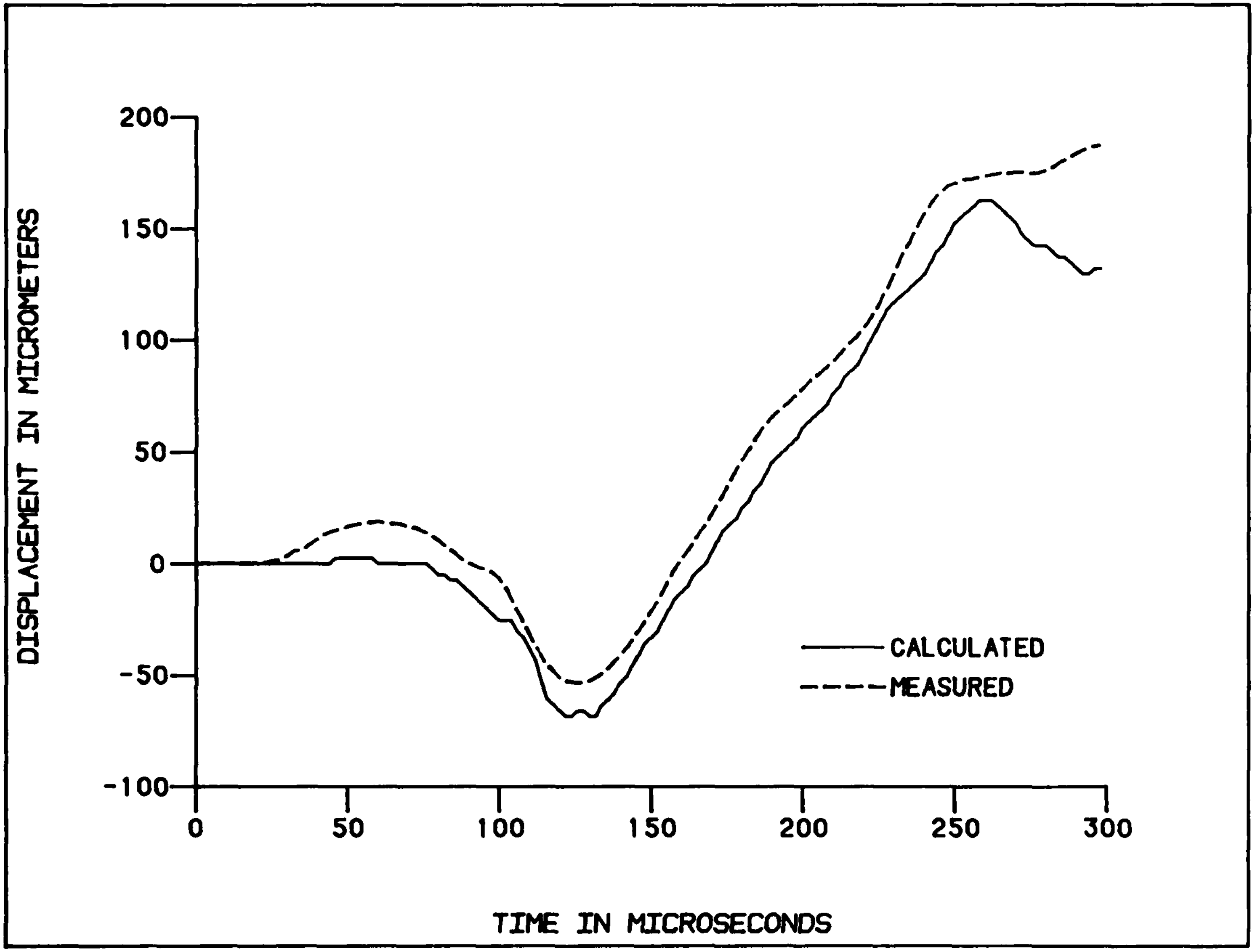

Figure 12. Axial displacement histories of 38 mm thick plate at 240 mm location for projectile impact velocity of 1012 m/s.

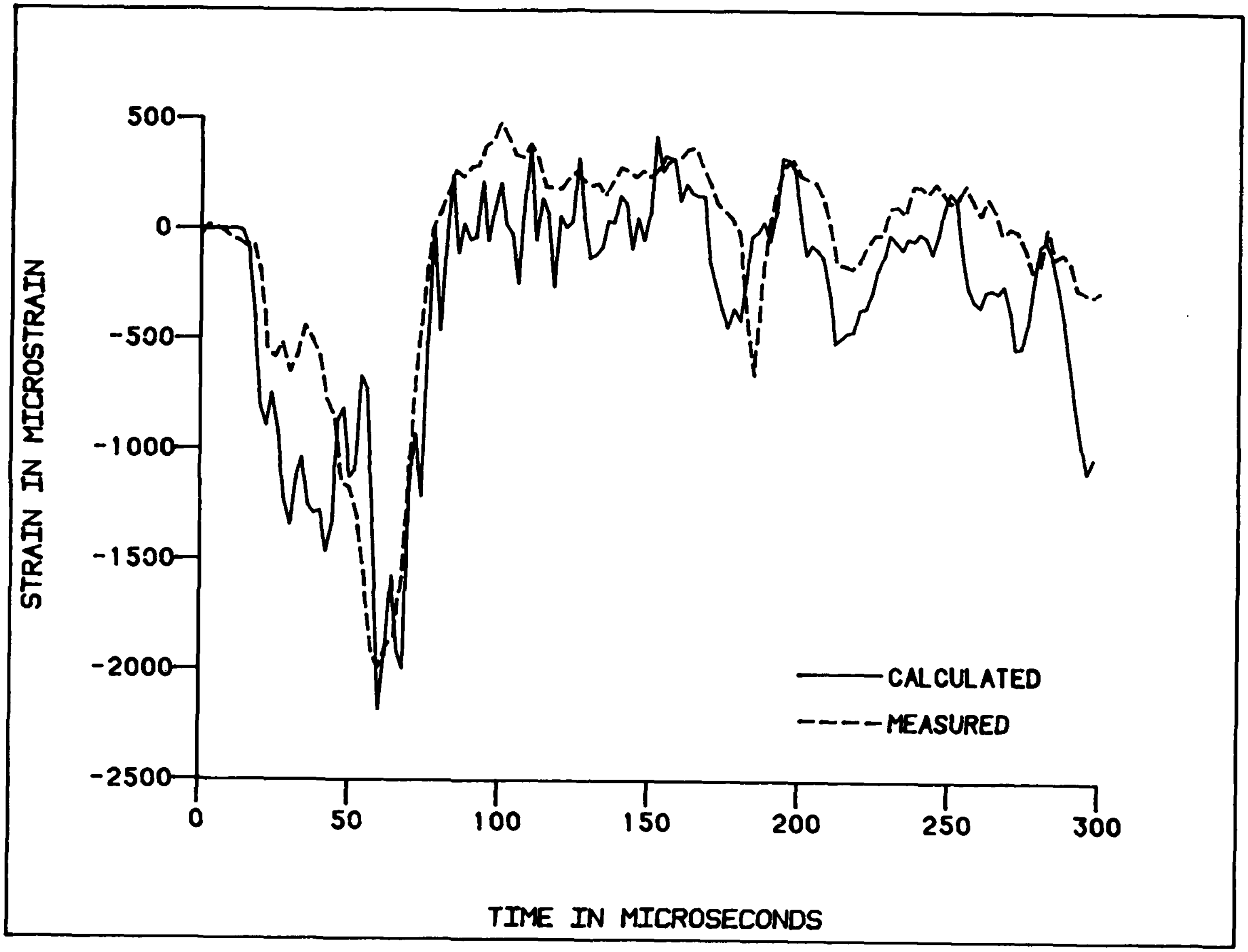

Figure 13. Radial strain histories of 38 mm thick plate at 100 mm location for projectile impact velocity of 1012m/s.

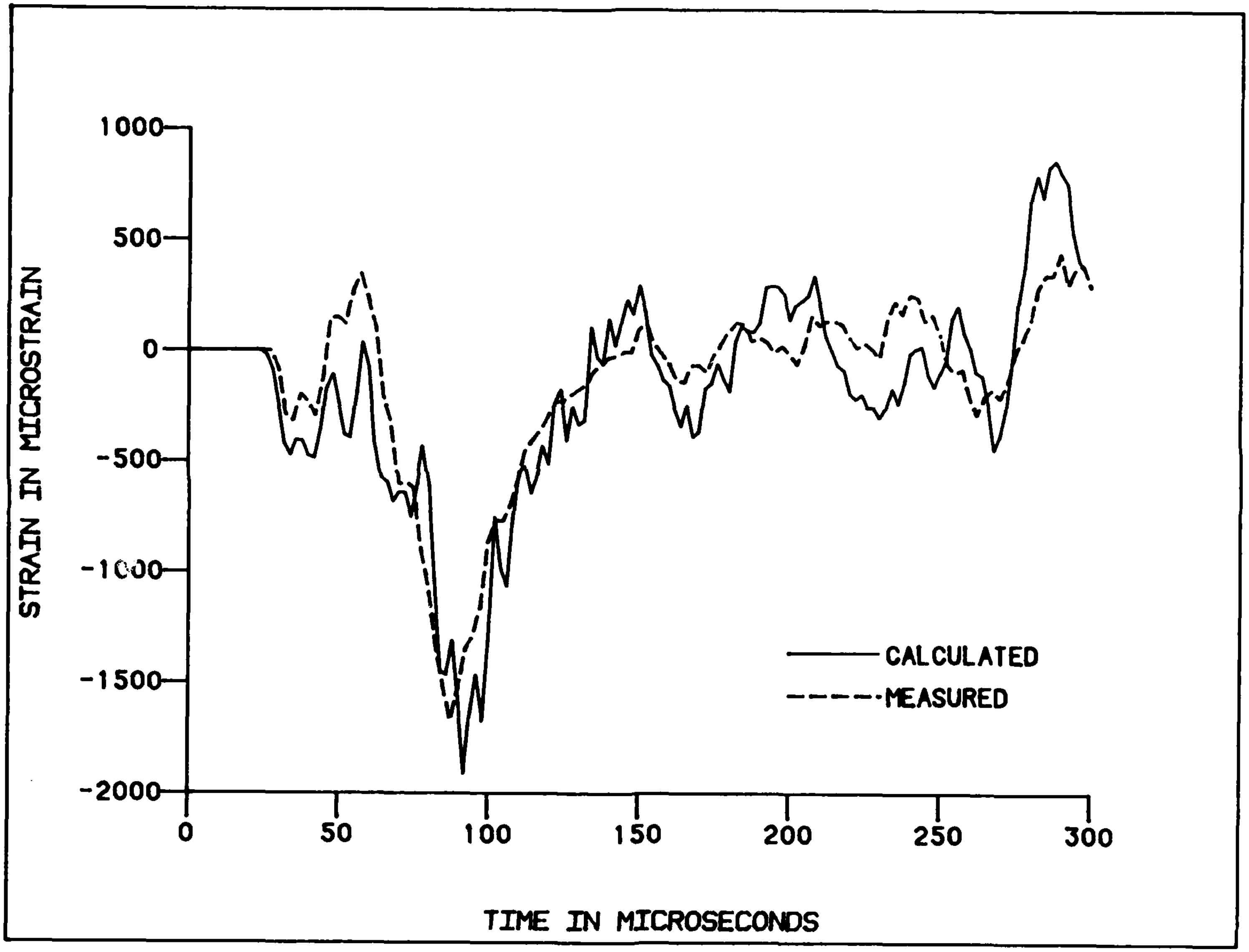

Figure 14. Radial strain histories of 38 mm thick plate at 170 mm location for projectile impact velocity of 1012 m/s.

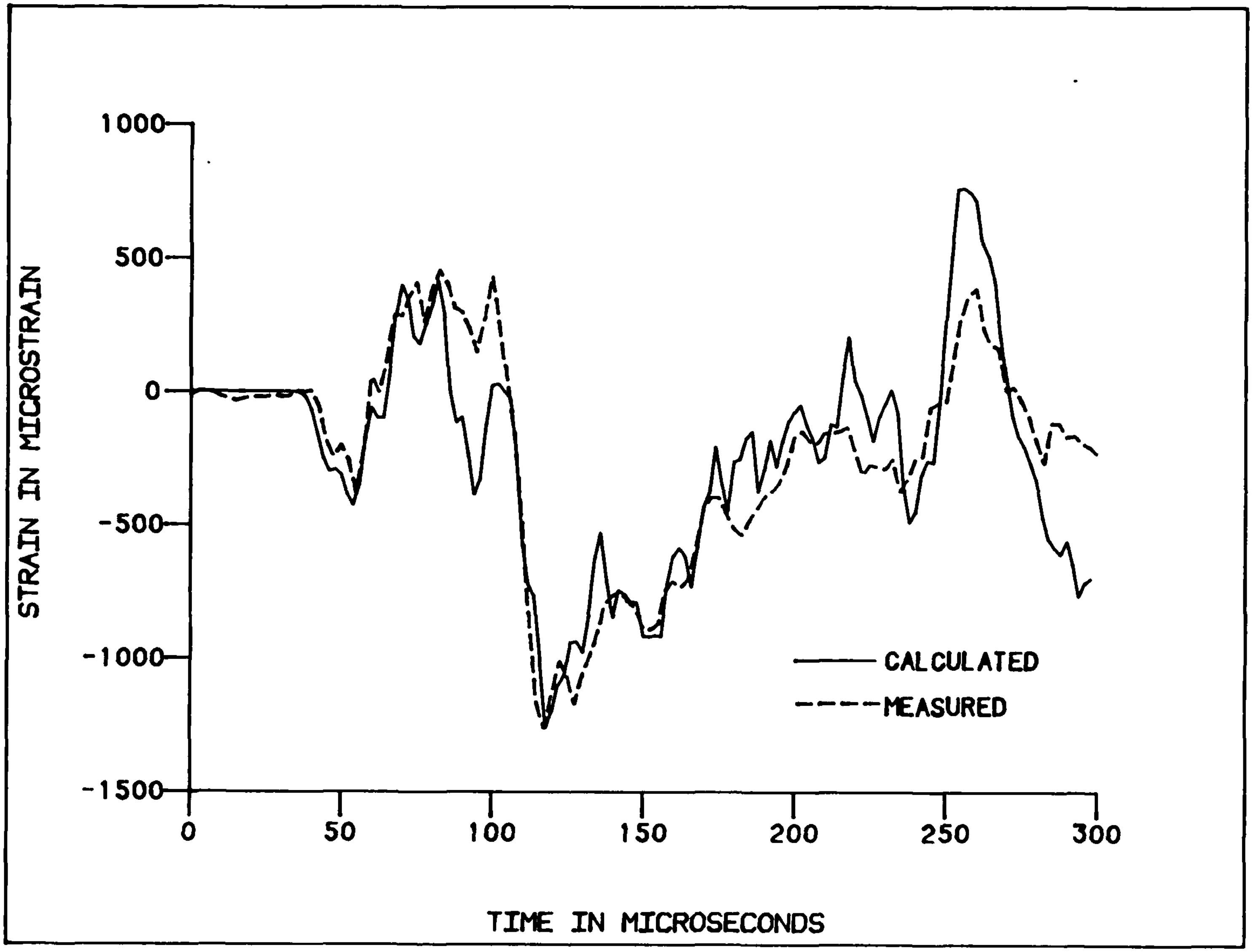

Figure 15. Radial strain histories of 38 mm thick plate at 240 mm location for projectile impact velocity of 1012 m/s.

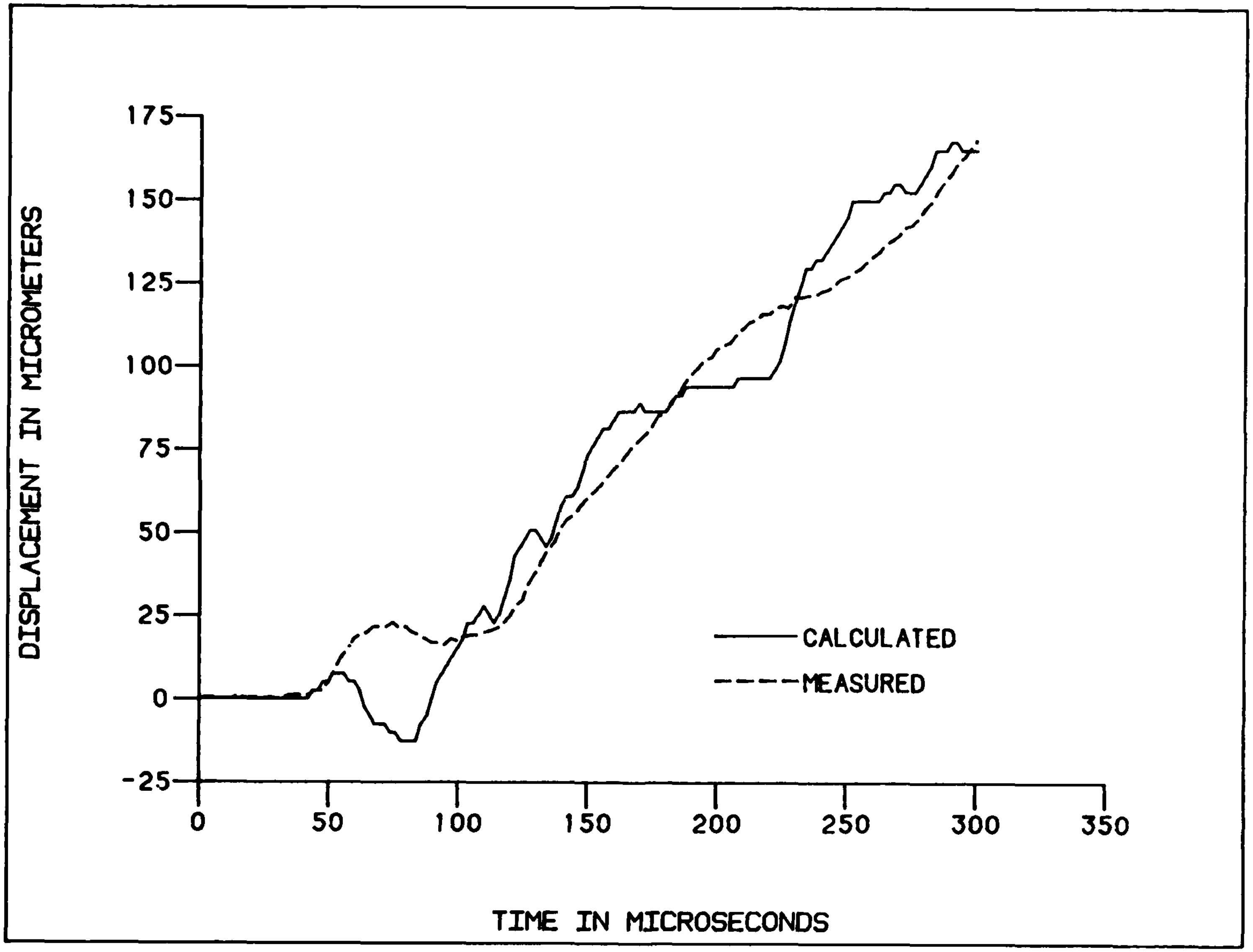

Figure 16. Axial displacement histories of 70 mm thick plate at 240 mm location for projectile impact velocity of 1508 m/s.

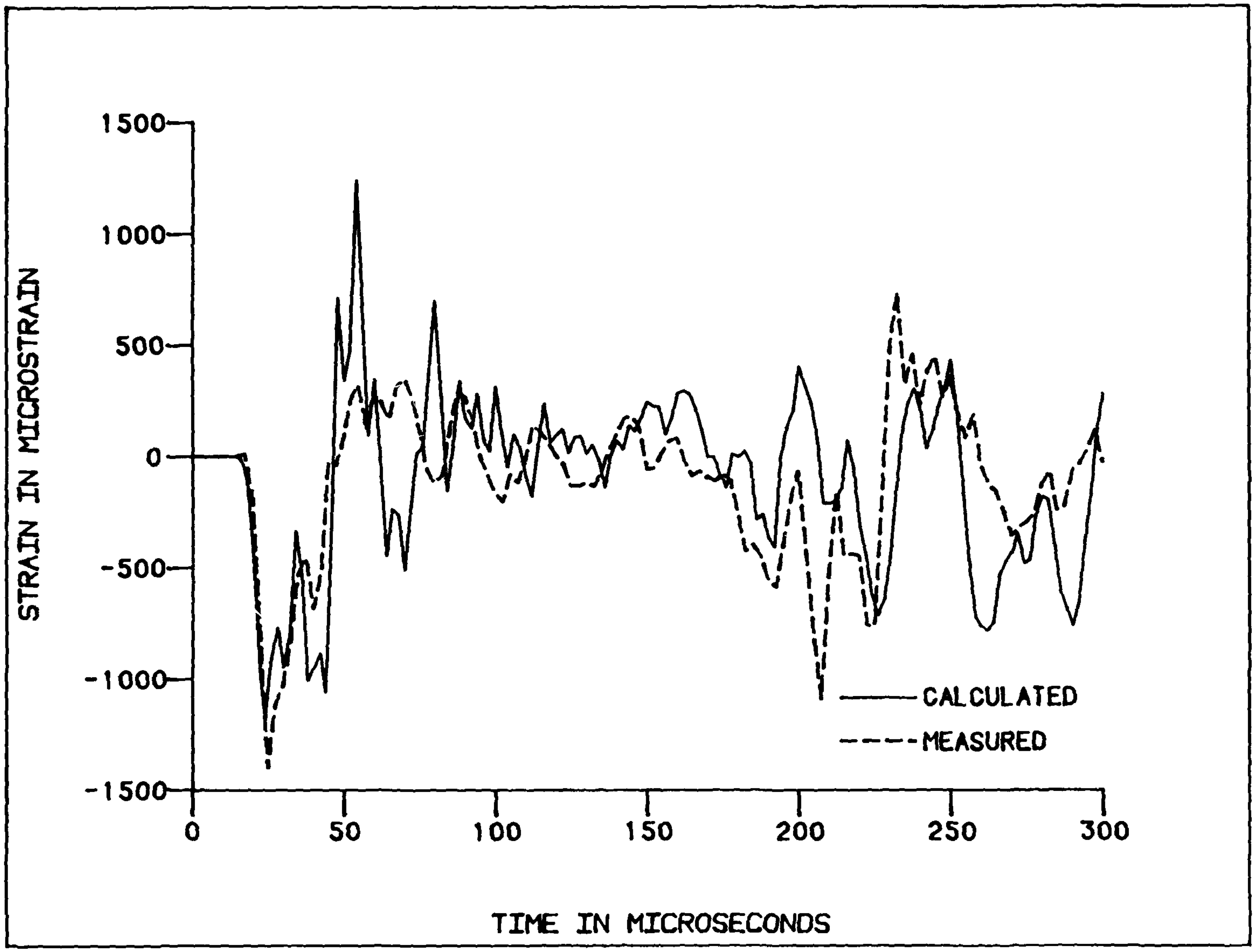

Figure 17. Radial strain histories of 70 mm thick plate at 100 mm location for projectile impact velocity of 1508 m/s.

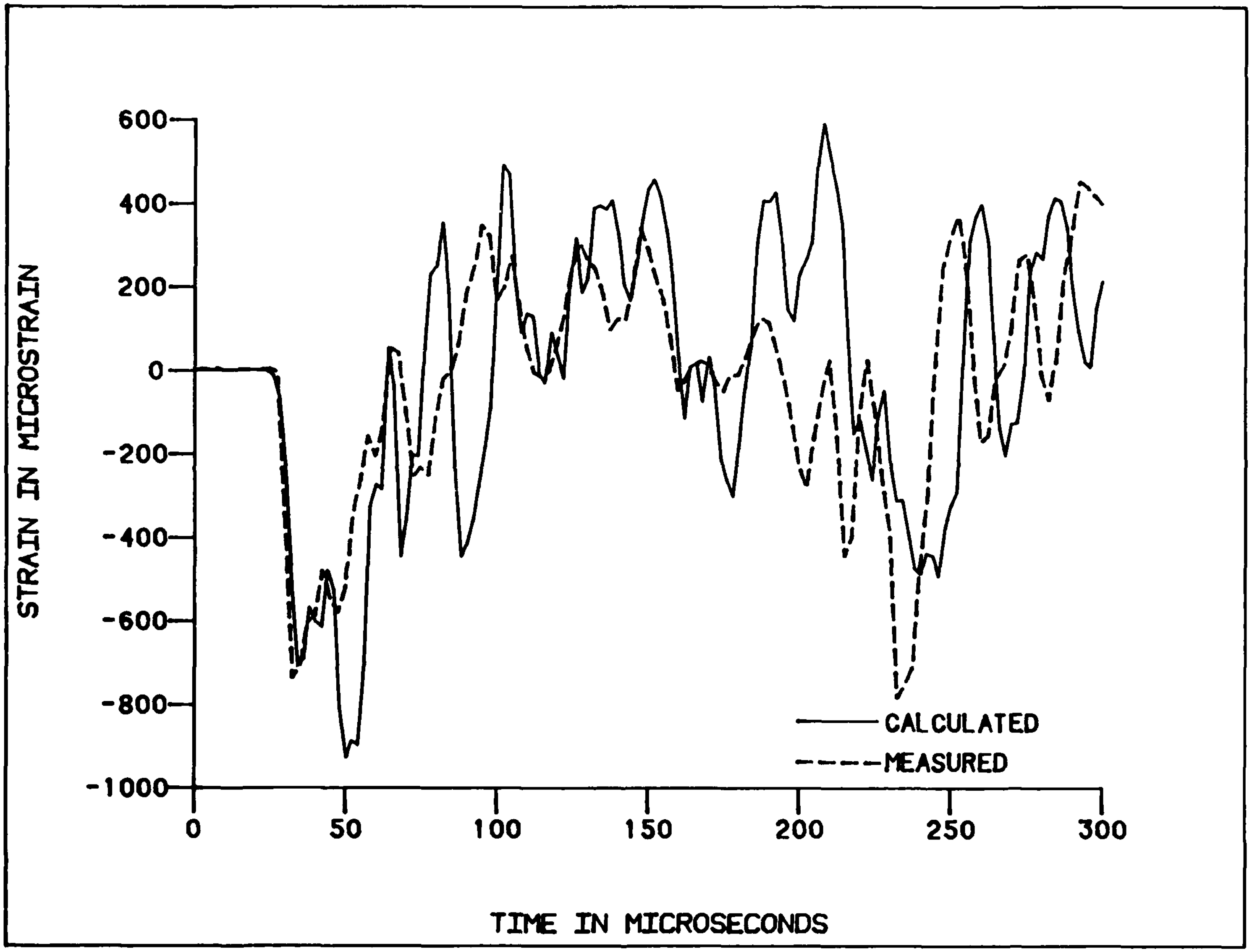

Figure 18. Radial strain histories of 70 mm thick plate at 170 mm location for projectile impact velocity of 1508 m/s.

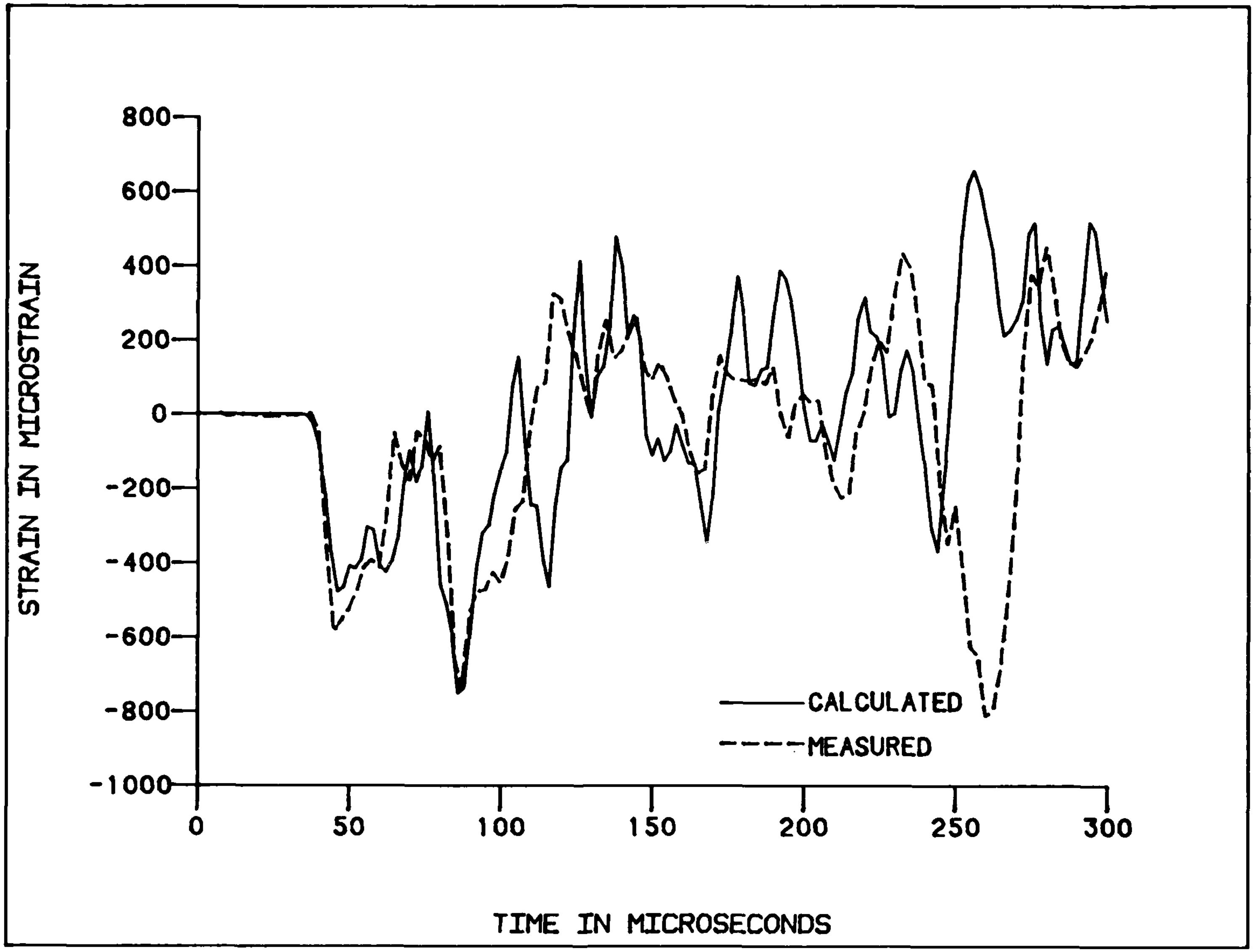

Figure 19. Radial strain histories of 70 mm thick plate at 240 mm location for projectile impact velocity of 1508 m/s.

As in the case of the measured displacements, the zero times for the measured radial strains were not at the time of impact. However, the zero time for the three strain measurements of each experiment was the same. For comparison purposes, the zero time of the measured data was determined by matching up the arrival of the dilation wave associated with the measured strain with that of the calculated strain at the 170 mm location and applying the same zero time adjusted to the other strain measurements. This procedure was followed for each impact velocity. The 170 mm location was chosen because the strain gage there was a semi-conductor type. The gages at the 100 and 240 mm locations were foil type and were subjected to possible electronic cross-talking. The agreement between the calculated and measured radial strains ranged from very good to excellent.

V. PREDICTED SHOCK ENVIRONMENTS

The axial acceleration histories calculated at the 0 mm and 240 mm locations on the back surface of the plates are shown in Figures 20 through 25. Figure 20 is the acceleration history at the 0 mm position for the 366 m/s impact velocity. The plot shows a frequency of approximately 170 kHz and a maximum peak acceleration of 500 kG's. Figure 21 is the acceleration history at the 240 mm position. The maximum peak acceleration is approximately 40 kG's, down by a factor of 10 compared to the maximum peak acceleration at the 0 mm location. Figure 22 is the acceleration history at the 0 mm position for the 1012 m/s velocity. Again the acceleration frequency is approximately 170 kHz and the peak acceleration is in excess of 3 MG's. Figure 23 is the acceleration history at the 240 mm position. Here the peak acceleration is approximately 150 kG's, down by a factor of 20. Figure 24 is the acceleration history at the 0 mm position for the 1508 m/s velocity. As before, the frequency is approximately 170 kHz. The peak acceleration is in excess of 2 MG's. This is lower than the peak acceleration for the 1012 m/s velocity because the higher velocity plate is 32 mm thicker. Figure 25 is the acceleration history at the 240 mm position. Here the peak acceleration is approximately 100 kG's, down by a factor of 20.

The maximum peak acceleration occurs during the first 50 μs at the 0 mm location for all three impact velocities. The calculated projectile impact duration times were 43 μs, 48 μs and 65 μs for the impact velocities of 366 m/s, 1012 m/s and 1508 m/s, respectively.

VI. CONCLUSIONS

1. The EPIC-2 hydro-code has calculated the responses of RHA plates to nonperforating ballistic impact which are in very good agreement with experimental results.

2. The predicted shock environment in the vicinity of the impact is characterized by a high frequency acceleration history (kHz range) with large peak accelerations (kG's to MG's range). However, it appears that the magnitude of the peak acceleration decreases rapidly as the disturbance propagates radially outward from the point of impact.

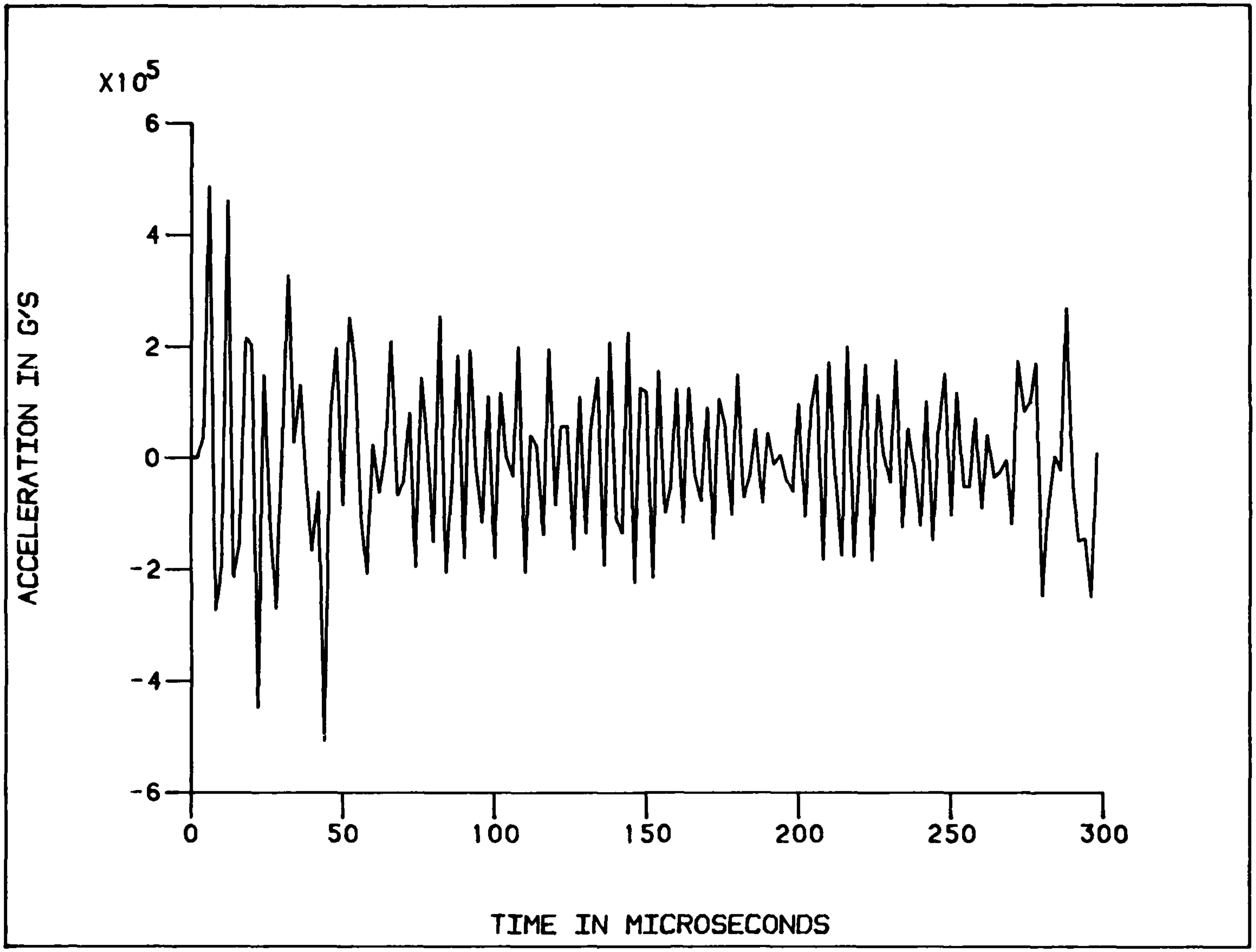

Figure 20. Axial acceleration history of 38 mm thick plate at 0 mm location for projectile impact velocity of 366 m/s.

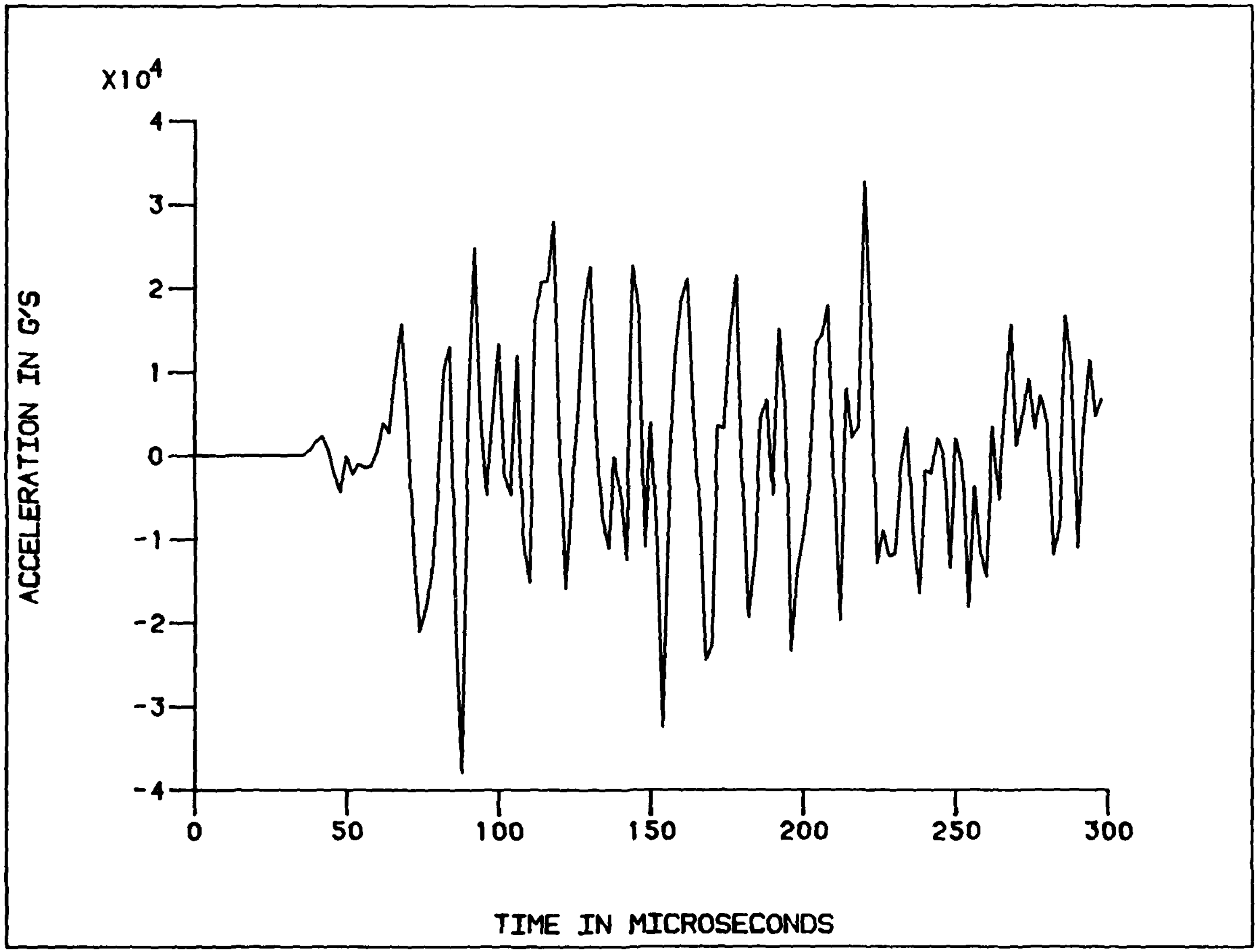

Figure 21. Axial acceleration history of 38 mm thick plate at 240 mm location for projectile impact velocity of 366 m/s.

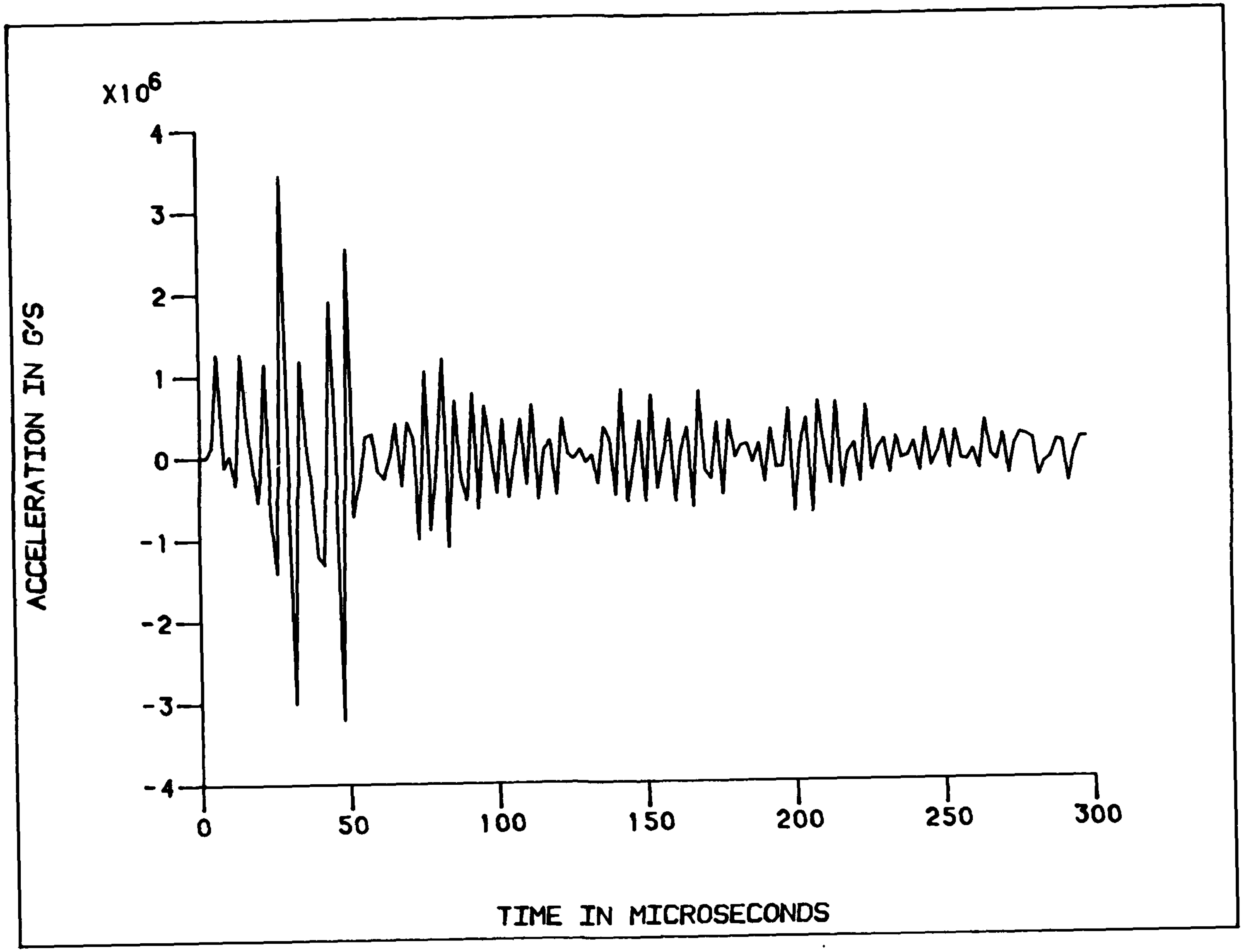

Figure 22. Axial acceleration history of 38 mm thick plate at 0 mm location for projectile impact velocity of 1012 m/s.

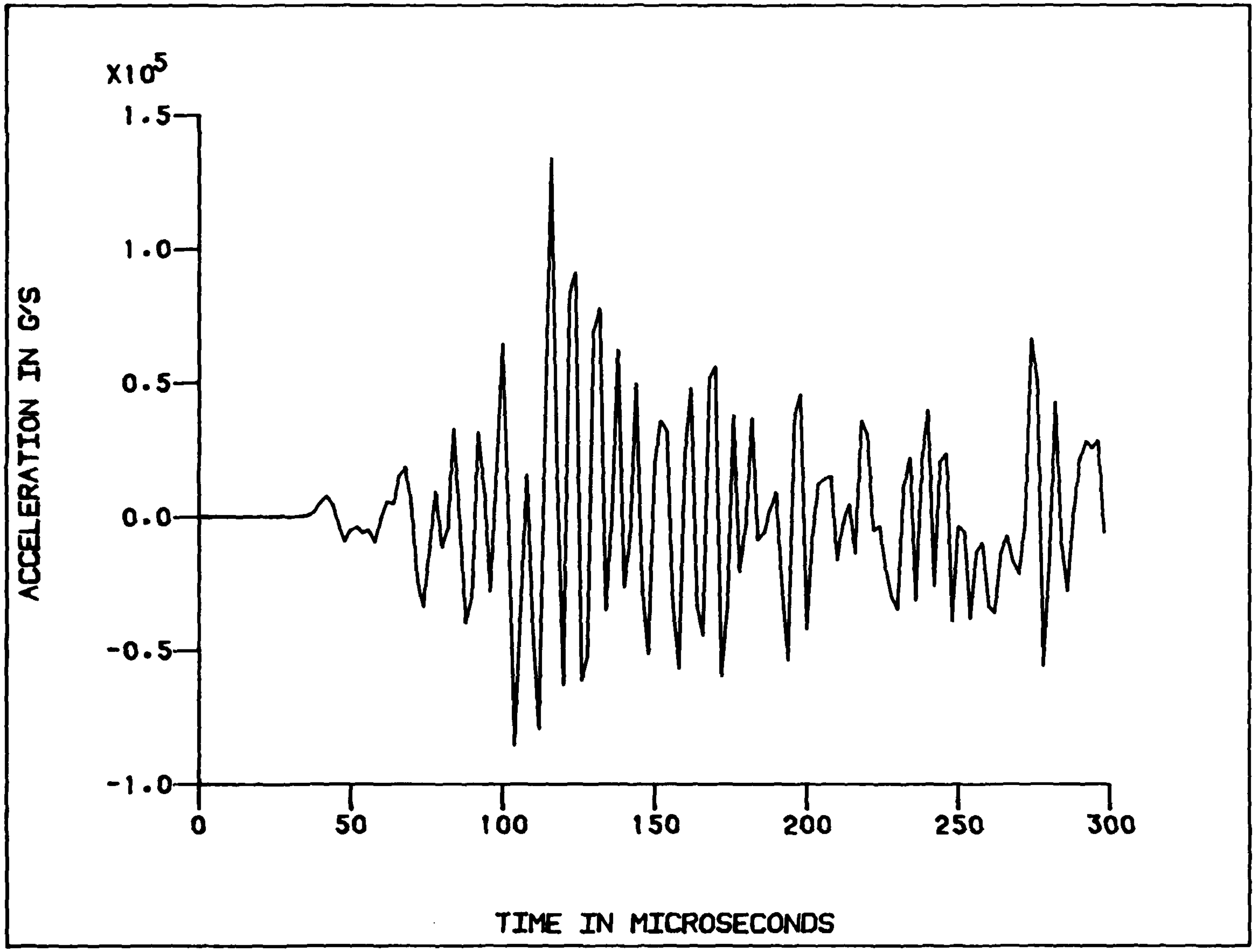

Figure 23. Axial acceleration history of 38 mm thick plate at 240 mm location for projectile impact velocity of 1012 m/s.

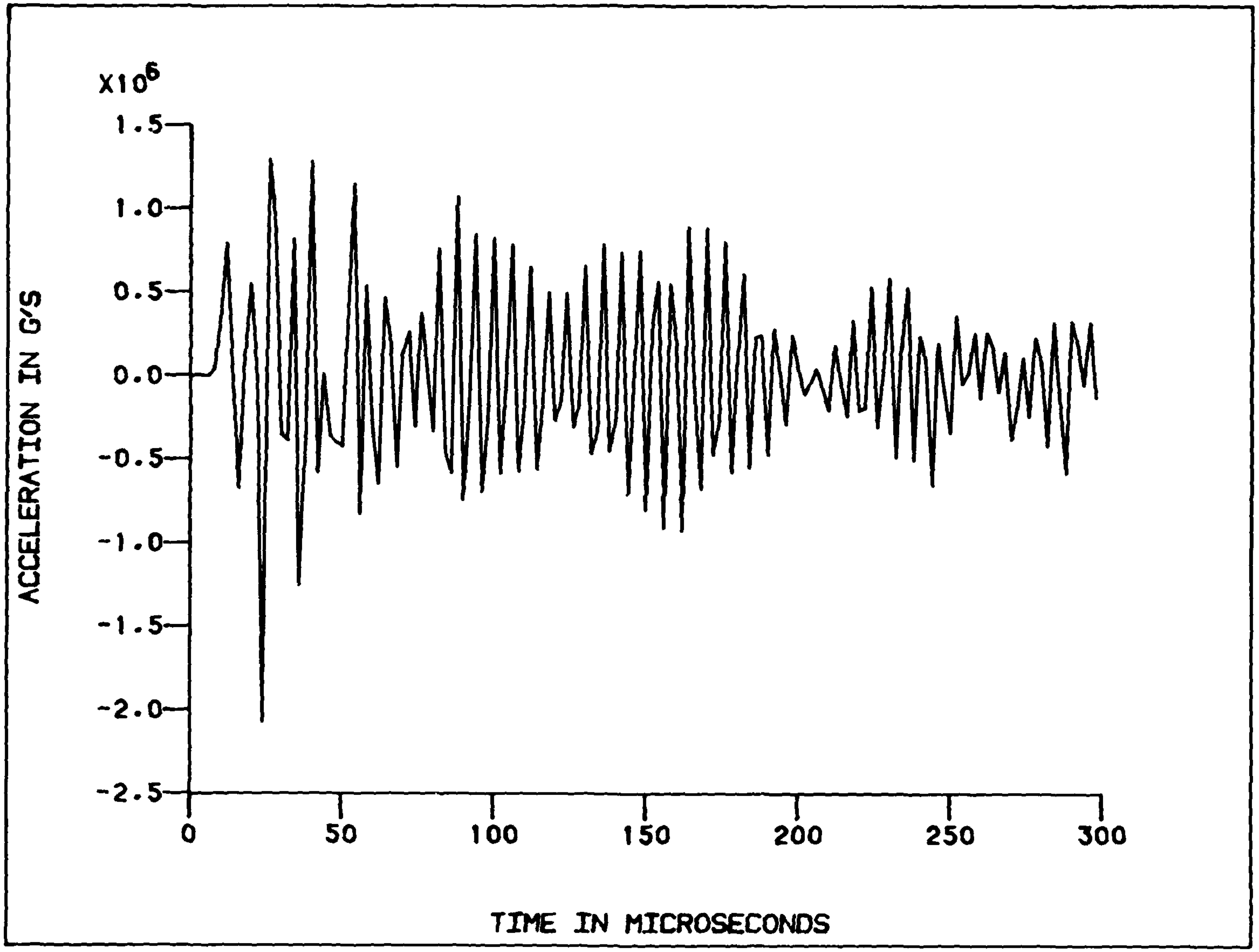

Figure 24. Axial acceleration history of 70 mm thick plate at 0 mm location for projectile impact velocity of 1508 m/s.

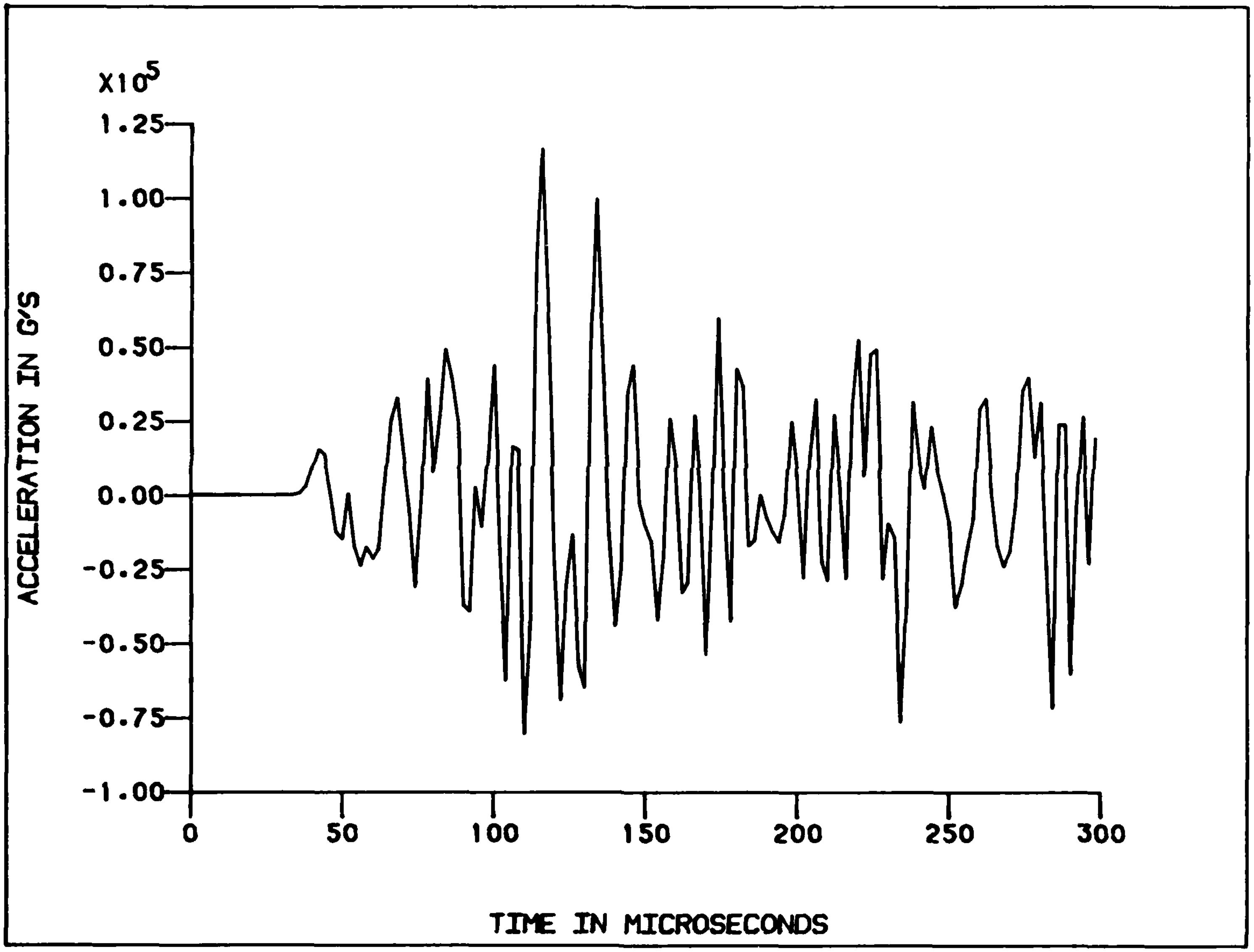

Figure 25. Axial acceleration history of 70 mm thick plate at 240 mm location for projectile impact velocity of 1508 m/s.

REFERENCES

1. Walton, W. Scott, Characterization of Ballistic Shock, USACSTA-6262, U.S. Army Combat Systems Test Activity, Aberdeen Proving, MD, November 1985.

2. Private Communications with W. Scott Walton, U.S. Army Combat Systems Test Activity, January 1986.

3. Johnson, Gordon R., EPIC-2: A Computer Program for Elastic-Plastic Impact Computations in 2 Dimensions Plus Spin, Contractor Report ARBRL-00373, U.S. Army Ballistic Resarch Labortory, Aberdeen Proving Ground, MD, June 1978.

DISTRIBUTION LIST

No. of Copies	Organization
12	Administrator Defense Technical Information Center ATTN: DTIC-DDA Cameron Station Alexandria, VA 22304-6145
1	HQDA ATTN: DAMA-ART-M Washington, DC 20310
1	Commander US Army Material Command ATTN: AMCDRA-ST 5001 Eisenhower Avenue Alexandria, VA 22333-0001
3	Commander Armament R&D Center US Army AMCCOM ATTN: SMCAR-TSS SMCAR-TDC SMCAR-SCM, Dr. E. Bloore Dover, NJ 07801
2	Director Benet Weapons Laboratory Armament R&D Center US Army AMCCOM ATTN: SMCAR-LDB-TL Dr. Joseph E. Flaherty Watervliet, NY 12189
1	Commander US Army Armament, Munitions and Chemical Command ATTN: SMCAR-ESP-L Rock Island, IL 61299
1	Commander US Army Aviation Research and Development Command ATTN: AMSAV-E 4300 Goodfellow Road St. Louis, MO 63120

No. of Copies	Organization
1	Director US Army Air Mobility Research and Development Laboratory Ames Research Center Moffet Field, CA 94035
1	Commander US Army Communications-Electronics Command ATTN: AMSEL-ED Fort Monmouth, NJ 07703-5301
1	Commander ERADCOM Technical Library ATTN: DELSD-L Fort Monmouth, NJ 07703-5301
1	Commander US Army Missile Command Research Development and Engineering Center ATTN: AMSMI-RD Redstone Arsenal, AL 35898-5500
2	Commander US Army Tank-Automotive Command ATTN: AMSTA-TSL AMSTA-RSS, Dr. J. Thompson Warren, MI 48397-5000
1	Director US Army TRADOC Systems Analysis Activity ATTN: ATAA-SL White Sands Missile Range, NM 88002-5022
1	Commandant US Army Infantry School ATTN: ATSH-CD-CSO-OR Fort Benning, GA 31905
1	US Army Development and Employment Agency ATTN: MODE-TED-SAB Fort Lewis, WA 98433-5000

DISTRIBUTION LIST

No. of Copies	Organization
10	Central Intelligence Agency Office of Central Reference Dissemination Branch Room GE-47 HQS Washington, DC 20502
2	Commander David W. Taylor Naval Ship Research & Development Center ATTN: Code 1740.4, R. A. Gramm S. L. Wang Bethesda, MD 20084
2	Commander Naval Surface Weapons Center ATTN: Dr. W. G. Soper Code G35, D. C. Peterson Dahlgren, VA 22448
2	Commander Naval Surface Weapons Center ATTN: Code R-13 Code U-11 Silver Spring, MD 20910
7	Commander Naval Weapons Center ATTN: Code 3181 Code 3261 Code 3171 Code 3835 Code 31804 Code 326 Code 3261 China Lake, CA 93555
1	AFATL/CC Eglin AFB, FL 32542
1	AFATL/DLODR Eglin AFB, FL 32542
1	AFATL/DLYV Eglin AFB, FL 32542
1	AFATL/DLODL Eglin AFB, FL 32542

No. of Copies	Organization
1	AFWAL/MLLN Wright-Patterson AFB, OH 45433
1	ASD/ENESS Wright-Patterson AFB, OH 45433
1	ASD/ENFEA Wright-Patterson AFB, OH 45433
1	ASD/XRP Wright-Patterson AFB, OH 45433
1	Lawrence Livermore Lavoratory PO Box 808 ATTN: Dr. J. O. Hallquist Livermore, CA 94550
1	Los Alamos Scientific Laboratory PO Box 1663 ATTN: Dr. R. Karpp Los Alamos, NM 87544
1	Sandia Laboratories ATTN: Dr. R. Woodfin Albuquerque, NM 87115
1	AAI Corporation PO Box 6767 ATTN: R. L. Kachinski Baltimore, MD 21204
1	Aerojet Ordnance Company 9236 East Hall Road Downey, CA 90241
1	Aerospace Corporation 2350 E. El Segundo Blvd. ATTN: L. Rubin El Segundo, CA 90245
1	Battelle Memorial Institute 505 King Avenue ATTN: Dr. G. E. Hahn Colombus, OH 43201
1	Computational Mechanics Associates 8600 LaSalle Road, Suite 614 Baltimore, MD 21204

DISTRIBUTION LIST

No. of Copies	Organization
1	FMC Corporation Ordnance Engineering Division ATTN: K. Ofstedahl San Jose, CA 95114
1	General Dynamics PO Box 2507 ATTN: J. H. Guadros Pomona, CA 91766
1	H. P. White Laboratory 3114 Scarboro Road Street, MD 21154
1	Honeywell, Inc. Government and Aerospace Products Division ATTN: Dr. G. Johnson 600 Second Street, NE Hopkins, MN 55343
1	Kaman Sciences Corporation PO Box 7463 Colorado Springs, CO 80933
1	Orlando Technology, Inc. PO Box 855 ATTN: D. Matuska Shalimar, FL 32579
1	SouthWest Research Institute Dept. of Mechanical Sciences ATTN: Dr C. Anderson 8500 Culebra Road San Antonio, TX 78228
1	University of Denver Denver Research Institute ATTN: R. F. Recht 2390 S. University Blvd. Denver, CO 80210

Aberdeen Proving Ground

Dir, USAMSAA
ATTN: DRXSY-D
DRXSY-MP, H. Cohen

Cdr, USATECOM
ATTN: DRSTE-TO-F

Cdr, USACSTA
ATTN: STECS-DA-I, S. Walton

Cdr, CRDEC, AMCCOM, Bldg E3516
ATTN: DRSMC-CLB-PA
DRSMC-CLN
DRSMC-CLJ-L

USER EVALUATION SHEET/CHANGE OF ADDRESS

This Laboratory undertakes a continuing effort to improve the quality of the reports it publishes. Your comments/answers to the items/questions below will aid us in our efforts.

1. BRL Report Number____________________ Date of Report__________

2. Date Report Received______________________________

3. Does this report satisfy a need? (Comment on purpose, related project, or other area of interest for which the report will be used.)_______________

4. How specifically, is the report being used? (Information source, design data, procedure, source of ideas, etc.)_______________

5. Has the information in this report led to any quantitative savings as far as man-hours or dollars saved, operating costs avoided or efficiencies achieved, etc? If so, please elaborate._______________

6. General Comments. What do you think should be changed to improve future reports? (Indicate changes to organization, technical content, format, etc.)

CURRENT ADDRESS

Name

Organization

Address

City, State, Zip

7. If indicating a Change of Address or Address Correction, please provide the New or Correct Address in Block 6 above and the Old or Incorrect address below.

OLD ADDRESS

Name

Organization

Address

City, State, Zip

(Remove this sheet, fold as indicated, staple or tape closed, and mail.)

END
DATE
FILMED
8-88
DTIC